

6. Implementation Action Plan

Based on the results of this project, the following Implementation Action Plan is meant to direct the Research Advisory Committee and MDOT executives in applying changes within department policy or practices. This guide provides an overview of the project and the problems it focused on changing. Additionally, the outcomes and potential values to MDOT are reviewed. Recommendations on how MDOT can incorporate UAV technology and information are provided.

6.1 Required Sections

Project Title: Evaluating the Use of Unmanned Aerial Vehicles for Transportation Purposes

Project Number: contract no. 2013-0067, authorization #1 (Z1), research no. OR13-008

Principal Investigator: Colin Brooks

Project Manager: Steve Cook, P.E.

Research Manager: Andre Clover, P.E.

Implementation Manager: _____

Technical Monitor: _____ (*if different from IM*)

Description of Problem:

With approximately 4 million miles of roads, 117 thousand miles of railroad, and 600,000 bridges, the transportation system in the United States is vast and complex (Landers 1992). With millions of people relying on the transportation network, the reliability, safety, and security of these infrastructure components is critical for the economic well-being of the country. Maintenance reports have indicated that nationwide, approximately 25 percent of bridges are structurally deficient or functionally obsolete. In addition, MDOT has previously reported that 12 percent of the state's 11,000 bridges are structurally deficient, with repair cost estimated to be \$140 billion (AASHTO 2008). In order to efficiently monitor and assess bridges and other transportation related components such as roadway assets, pump stations, and traffic conditions, new advancement in technologies that can minimize costs and periods of inspection need to be assessed and incorporated into monitoring techniques.

Current bridge assessment techniques including coring, conductivity, pavement sounding using acoustics (i.e. chain dragging and hammer soundings) and ground penetrating radar can be tedious, time consuming, labor intensive, operator dependent, and cost prohibitive. These tests often include visual inspections, creating results that are operator dependent. Additionally, these tests often require road closures, which increase safety concerns for both inspection

teams and drivers. Therefore, any advancement in technology could greatly enhance transportation asset inspection and maintenance procedures.

Advancements in the field of remote sensing using UAVs can provide transportation agencies with ready, rapidly deployable systems capable of collecting imagery and related data in both challenging and wide-open spaces. For the purposes of this research and demonstration project, multiple UAVs ranging in size (i.e. micro-UAVs to mid-sized ones with 3-foot wingspan), type (i.e. quadcopter, hexacopter, and aerostat/blimp), and flight times were used to assess bridge health, confined space conditions, roadway asset types, and monitoring of traffic. The overall goals for this project were to demonstrate and enhance UAV capabilities to meet the needs of MDOT, often at resolutions higher than what is currently available, and to evaluate the effectiveness and quality of data collected by the UAV systems. By successfully completing these objectives, MDOT would have the capability to enhance their inspection methods, potentially creating a less-costly assessment procedure that also creates a safer working environment for assessors and the general public.

Major Discoveries:

For this project, inspection methods using UAVs showed significant promise in each of the main areas of interest (bridges, confined spaces, traffic monitoring, and roadway assets). The following paragraphs review the major accomplishments and discoveries made within each area; additional detail is the major content of the project final report.

Bridge Condition Assessment:

Using a Bergen Hexacopter equipped with different sensors (FLIR Tau2-based thermal camera, Hokuyo LiDAR, and a 36-megapixel Nikon optical camera) during different flights, the UAV-based platform was able to collect imagery that highlighted surface (i.e. spalls and patches) and sub-surface (delamination) defects on two separate bridges in Livonia, Michigan that were part of the major Interstate-96 reconstruction project. It is important to note that traffic operations were closed off to the bridge during data collection, but that it is possible to collect UAV-based imagery without having to require closures. Optical imagery collected by the sensor was reconstructed in 3-D modeling software to create an orthophoto and digital elevation model (DEM) with a resolution of 2.5 millimeter. The DEMs for each bridge were also processed through a spall detection algorithm, which automatically digitized changes in elevation of the bridge deck that represents a spall. An overall percent spall value for the entire bridge was then calculated. Delaminations were detected using thermal imagery, due to the fact that these defects have a different temperature than their surroundings. Similar to the optical camera, the FLIR Tau2 collected imagery as it was flown over the bridge. Images were georeferenced in ESRI's ArcMap also processed through an automated detection algorithm, which provided total area and percentage of delaminations. LiDAR data was successfully collected via UAV for one of the study bridges, and the data processing improvements from Simultaneous Location and

Mapping (SLAM) algorithms were used to enhance the quality of the LiDAR point cloud data for more accurate 3D model creation of bridges and other transportation features.

Confined Spaces – Culverts and Pump Stations:

Through the use of multiple mini-quadcopters that were equipped with onboard camera and video recorders, the project team was successfully able to conduct short flights in confined spaces with real-time video display. For culvert analysis, initial results indicated that a more stable platform with onboard lighting needs to be used to obtain quality data. During sample flights, the UAV platform experienced ground effect, a phenomena that occurs when an aircraft is close to the ground and the propellers end up displacing air beneath it, causing the air pressure below the aircraft to increase. This results in increase lift on the aircraft at low altitudes. Similar phenomena occur when the aircraft is near a wall or ceiling. Although more testing is needed in order to collect high quality data, captured video proved that UAV-based inspections conducted before a person enters a culvert is possible.

For pump station inspections, live video and still images were displayed and captured. Both types of data could be saved on a memory card for later viewing, or broadcast live to a cellular device. The main obstacle was flying through the pump station's entrance hatch, an area of approximately 9 square feet. Similar to the phenomena experienced in a culvert, the UAV experienced ground effect as it passed through the entrance hatch. In order to solve this, pilots decreased the throttle, therefore lowering the device quickly and then increased the throttle immediately to prevent the UAV from crashing into the ground. Live video highlighted multiple features within the pump station, including conditions of pipes and levels of water. Helping provide information on the safety level of a pump station could prove highly beneficial for a pump station inspector, before having to physically enter the area.

Traffic Monitoring:

Project tests and demonstrations in using a blimp for traffic monitoring proved successful, but also highlighted the need for a stabilizing mount for the sensor. Although live video was captured and transmitted to a handheld tablet device, the video was unstable and of low quality due to wind acting against the tethered blimp. Additional flights and testing incorporated the use of a gimbal device, which promoted a steadier sensor with limited disruptions. As expected, the quality and stability of video collected during these additional flights were much better and were transmitted to USTREAM (www.ustream.tv), a broadcasting service that promotes engaging global audiences with live content. Videos broadcasted to USTREAM can be viewed in real-time, and are saved for future viewing opportunities. Videos collected during this project can be viewed at www.ustream.tv/channel/mtri. The quality of video collected using the gimbal device is similar to typical traffic camera quality of video. However, the benefit of using a tethered device as compared to a traffic camera comes from

the fact that the blimp is a temporary, non-stationary structure and can be deployed for events of interest.

Roadway Asset Detection:

A computer-vision based method for detecting, tracking, and identifying specific roadway assets (often called “roadway assets” by asset managers) was developed and demonstrated as part of this project. These methods used image classification, tracking of asset features between video frames, and an initial demonstration with a set of known test imagery. The demonstration was then extended to show how stop signs, handicap parking signs, and traffic lights could be detected using UAV-based data collection. Other assets can be detected by providing example images to the classifier software, so expansion of roadway asset detection if possible.

MDOT has previously funded research related to roadway asset detection (see “Monitoring Highway Assets with Remote Technology”, project no. OR10-030, report number RC-1607, at http://www.michigan.gov/documents/mdot/RC-1607_466453_7.pdf), but this was focused on comparing vehicle-based and manned helicopter-based mobile asset data collection to traditional manual methods. Our project focused instead on the potential for UAV-based roadway asset detection and data collection. The demonstration showed promise for a UAV-based mobile asset data collection concept and could be developed further.

How the information will be used in MDOT:

UAV data has the potential to be widely used within MDOT. Already, staff from MDOT Survey Support has expressed interest in being able to use and share the types of high-resolution imagery and digital model data that can be produced from UAV flights with appropriate cameras. MDOT Bridge Management team members, including inspectors and bridge managers, are logical consumers of the bridge condition data derived from optical and thermal data sources, as the percent spalled and percent delaminated for bridge deck surfaces are already information that is needed in current bridge inspections. Engineers in charge of construction site monitoring could use lower and higher-resolution imaging to monitor progress in construction, estimate the changing volume and height of gravel and fill piles. Traffic engineers and operations managers can use the ability to quickly deploy mobile, airborne traffic monitoring cameras using a blimp to extend the reach and capability of MDOT’s traffic camera network, without the need to install new permanent infrastructure. When MDOT helps with emergency response scenarios, combinations of UAV platforms and the traffic blimp can provide real time and near-real time information on developing situations where overhead photos would be valuable.

The typical costs of equipment purchased or otherwise made available for this project are included in various appropriate sections of this report. Formal cost/benefit analyses were not

part of this project, but representative cost numbers are made available so that MDOT can have an understanding of the current hardware and software costs experienced by the Michigan Tech team. Hardware and software can change rapidly, with the general trend being lower costs with greater capabilities, with new versions sometimes released several times a year. MDOT may choose to purchase equipment and software for its own use in some areas, such as traffic monitoring. The Survey Support staff may want to process imagery data sets in house using software tested in this project to create custom products needed by MDOT.

However, implementation for more service-type data needs, such as bridge inspections, may be more suited to collection and processing via third-party vendors, especially where MDOT is already works with the private sector. For example, aerial imagery collections and some bridge inspections are completed through partnerships with private companies. Once more widespread commercial usage of UAVs is enabled through new FAA rules, then these types of firms may start offering UAV-based data collection services to MDOT and other transportation agencies, providing another implementation option to MDOT.

Value Added to MDOT:

Through careful evaluation and conducting multiple tests in various locations, the project team has demonstrated how UAV capabilities can provide quality data in both challenging confined areas and more wide-open spaces. The overall goals of providing MDOT with demonstrations of UAV capabilities to meet the transportation agency's needs and to evaluate the effectiveness and quality of collected data were accomplished. MDOT is now gaining access to advanced technologies that can provide cheaper and safer ways of collecting critical operations and maintenance information.

For bridge condition assessments, processing of optical, thermal, and digital elevation imagery and models proved the UAVs were able to produce spall and delamination detections that are comparable to current hammer and chain drag techniques. Results from these analyses indicated that using UAVs to collect data will produce quality outputs, which in turn will create safer working conditions by reducing the time onsite workers need to spend on highly traveled roads. Additionally, the area and percent spall or delamination can be automatically calculated. In order to conduct this type of analysis, MDOT will have to train qualified onsite workers to fly the UAV, or acquire the capability as a third-party service. For an MDOT employee with prior training in how to fly UAVs, training can be accomplished in approximately one day, as the hexacopter is a relatively stable platform that is easy to control. However, it would take an extended amount of time to train an employee with no prior experience in flying UAVs. The total amount of time that it would take to complete a bridge condition UAV flight, from setup to tear-down is approximately one hour. In addition, this type of analysis would diminish costs

associated with bridge inspections, such as lane closures and potentially also the amount of personnel time needed to conduct a traditional inspection (i.e. labor costs).

Through inspection of data (i.e. videos and still images), the project team demonstrated that using UAVS for confined space inspection is practical. Although video cameras pre-equipped on these small-sized UAVs produce video outputs of lower resolution than the other sensors tested during this project, pipelines, water levels, and other features of interest are still visible and can provide MDOT with an ideas into the conditions that exist within a confined space without placing an inspector in the space. It is also important to note that even though UAVs can help indicate current environmental conditions, it will still often be necessary for an MDOT to enter the confined space in order to make desired improvements or repairs, but they can do so with more information on the safety conditions inside that confined space. Training a UAV operator how to fly indoors would mean additional hours will be necessary, so third-party service options may be a desirable option. The time required to fly a micro-UAV indoor is relatively minimal, but requires the pilot to be aware of and know how to correct for phenomena such as ground effect and how the aircraft reacts to flying near sidewalls or ceilings. Additionally, the pilot must learn how to maneuver the UAV through an entrance hatch in order to avoid losing the aircraft in water present in a pump station. Similar to bridge evaluations using UAVs, this type of analysis could also result in diminished initial inspection costs with increased safety.

Traffic monitoring through the deployment of a low-cost tethered aerial system has demonstrated how an UAV is capable of operating where non-permanent infrastructure is desirable. Testing has also indicated that video resolutions from this system closely resemble the current resolution capabilities of permanent traffic monitoring cameras. Scenarios could include major events such as sporting, concert, weather, and emergency response events. If planned monitoring events are expected to occur for a longer period of time, an electrical source would need to be incorporated either onboard or as part of the tethering system. With the sensor collecting and transmitting live imagery or video over a 4G network, MDOT is capable of viewing of the video stream virtually at any location that contains Internet access. Training a pilot to control a blimp UAV is very minimal and only requires the pilot to be aware of surroundings and locations where the UAV can be tethered to, along with typical tethered blimp safety rules. Incorporating this type of sensor is designed to minimize construction and maintenance costs to install permanent monitoring infrastructure.

Checklist:

The following checklist provides a summary for MDOT on understanding of the type of results achieved during this project and what items or actions are needed to implement these results (Table 6.1 A).

Table 6.1 A: Implementation Action Plan checklist

Results achieved through this research (check all that apply)		Items/Actions needed to implement results (check all that apply)	
X	Knowledge to assist MDOT	X	Management decision
	Manual change	X	Funding
	Policy development or change	X	Training
X	Development of software/computer application	X	Information technology deployment
X	Development of new process	X	Information sharing
X	Additional research needed		Other (specify)
	Project produced no usable results		
	Other (describe)		

6.2 Recommendations for Future Research

Additional potential tasks for the “Evaluating the Use of Unmanned Aerial Vehicles for Transportation Purposes” MDOT research project, Contract/Authorization No. 2013-067, Authorization Project No. 1, OR No. OR13-008.

Based on the proven technology capabilities and success in data collection and processing, the project team has developed additional recommendations for future research that also incorporate UAV technology in data collections. The following sections describe potential applications that the project team deem practical for future studies that MDOT may find interest in.

The Michigan Tech project team has been working with MDOT on demonstrating applications of UAVs for helping with critical transportation infrastructure and traffic monitoring needs. In the current project, we have been developing applications focused on confined space inspection, traffic monitoring, bridge condition assessment, and roadway inventory. We believe that we have shown sufficient progress to potentially merit completing additional tasks for MDOT under an extended timeline and budget total. Based on our progress so far, we are recommending the following additional deliverables to be added to our current research project with MDOT:

1. Operations (traffic monitoring for a TOC) and Maintenance (i.e. PDRP, TAMS, PBOS) uses and demonstrated cost savings as a result of this technology.
2. Provide data collection from UAVs to the MDOT Data Use Analysis and Process (DUAP) project that meets the low latency delivery and data format requirements.
3. A formal demonstration of crash scene reconstruction imaging.
4. A demonstration of slope stability assessment (for example, for retaining walls).
5. A demonstration of the capabilities to complete aerial imaging to meet MDOT mapping and construction monitoring needs.
6. A report that describes and recommends optimal methods to store and distribute potentially large imaging and 3-D surface datasets created through UAV-based data collection.
7. Enhanced testing of UAV-based thermal imaging for bridge structural integrity and geotechnical assets.
8. A demonstration of high-accuracy simultaneous thermal/video/LiDAR measurement using a high-fidelity sensor-fused UAV positioning approach.

6.2.1 Operations (traffic monitoring for a TOC) and Maintenance (i.e. PDRP, TAMS, PBOS) uses and demonstrated cost savings as a result of this technology.)

A significant part of helping operations and maintenance priorities for MDOT is understanding traffic flows and being able to response quickly to changing events and real-time conditions. To help with this need, the project team developed and demonstrated a relatively low-cost traffic monitoring blimp. Lab testing was performed at MTRI in Ann Arbor, where a good view of US-23 could easily be obtained, and a longer demonstrating was completed during four days of the ITS World Congress out at the Belle Isle as part of the Technology Showcase. The traffic monitoring blimp operated for several hours a day, with over seven hours of video being recorded. Video was sent near-live using the camera's 4G Verizon connection and the USTREAM web service to computers and the south video wall at the MDOT TOC inside the Cobo Hall Exhibition area during the World Congress. The USTREAM service introduced a 10-15 second delay; using MDOT's traffic camera communications network would be an alternative. The blimp setup consisted of \$1500 of hardware with an \$800 advertising blimp, a \$400 Samsung digital camera, and a \$300 gimbal (for stabilizing the camera). A single \$180 standard-sized tank of helium was enough for four days of continuous blimp inflation including top-offs and operations of three to eight hours a day during the ITS World Congress.

Capabilities provided by this low-cost blimp technology could also help with maintenance issues, including providing data for MDOT's Property Damage Reclamation Process (PDRP), the Transportation Asset Management System (TAMS), and the Performance-Based Operational System (PBOS). The potential for contribution to these needs should be assessed as part of a Operations and Maintenance future research effort.

Through this demonstration, we are now recommending that MDOT expand this effort into a series of working demonstration that feeds video from into an MDOT facility, such as the Southeast Michigan Transportation Operations Center (SEMTOC). The project's State of the Practice report reviewed two larger systems able to deploy for longer periods of time with a stronger tether and operate in stronger winds than the \$800 advertising blimp, without having to go to the level of the "Blimp in a Box" system recently adopted by Ohio DOT that cost \$180,000 (<http://www.dispatch.com/content/stories/science/2014/07/20/blimp-in-a-box.html>). A Kingfisher aerostat (see Figure 6.2.1 A) costs approximately \$6100 plus appropriate camera system such as the Samsung 4G plus helium to start operations (see <http://www.aerialproducts.com/surveillance-systems/kingfisher-wind-capable-aerostat.html> and <http://www.aerialproducts.com/aerial-photography-systems/balloon-aerial-photography-systems.html>). We recommend that MDOT test one or more these enhanced platforms, using a similar cell-network capable camera system, but with integration with MDOT's capabilities to transmit and display traffic camera data. The USTREAM-type widely available web video

capability could continue to be tested as a method of making the blimp-based video data easily available for demonstrations.



Figure 6.2.1 A: A Kingfisher aerostat with sail that helps keep the aerostat from rotating in the wind and provides lift. The project's Samsung 4G camera or similar system could transmit near-real time video from this platform to a TOC.

For this additional task deliverable, we would:

- Recommend an enhanced traffic monitoring blimp with greater weather, deployment time, and payload capabilities, but still with reasonable cost.
- Work with MDOT to integrate video transfer capabilities into secure MDOT networks for displaying data into a TOC.
- Demonstrate a blimp-based traffic monitoring session at appropriate MDOT priority locations with a TOC for two or more time periods of approximately one week or longer.
- Summarize recommendations, testing, and results in a blimp-based traffic monitoring report focusing on a guidance document that provides practical implementation for public agencies.
- Assess how a blimp-based system could help provide data to meet maintenance data needs for MDOT efforts such as PDRP, TAMS, and PBOS.

6.2.2 Provide data collection from UAVs to the MDOT Data Use Analysis and Process (DUAP) project that meets the low latency delivery and data format requirements.
MDOT's ongoing efforts in evaluating, testing, and deploying connected vehicle technologies has made it a leader in becoming "the agency of the future" (a title of an MDOT talk at the recent ITS World Congress). Part of that is the Data Use Analysis and Process (DUAP) project, which is focused on "evaluating uses and benefits of connected vehicle data in transportation

agency management and operations" (https://www.michigan.gov/documents/mdot/08-31-2012_VII_DUAP_Project_Summary_Report_444701_7.pdf). UAV-based sensing has the capability to provide useful data that complements connected vehicle data. This could include traffic monitoring data (described above) and pavement defect and condition assessment data (similar to the bridge condition demonstration). Particularly useful is the capability of UAVs to provide imagery data on a low-latency basis due to their rapid deployment .

For this additional task deliverable, we would:

- Work with MDOT to define how rapid UAV-based sensing could provide low-latency data for connected vehicle DUAP project efforts in required data formats.
- Demonstrate how UAVs could collect needed data for the DUAP project.
- Summarize recommendations, testing, and results in a DUAP data collection report to help MDOT understand the contributions that UAV-based sensing can make to this critical program area through practical implementation.

6.2.3 A Formal Demonstration of Crash Scene Reconstruction Imaging

For crash scene reconstruction, our team has completed three example imaging demonstrations: 1) for the MSP in August of 2013, 2) for the Southeast Oakland County Crash Investigation Team (SOCCIT) in April of 2014, and 3) as part of the Mock Incident for the ITS World Congress Emergency Response Day in September of 2014. In the MSP demo, we showed how one could rapidly collect imagery from a small quadcopter so that a member of the MSP Crash Scene Evaluation team could more easily measure crash scene information taken. MSP is currently evaluating where it would like to move with this technology, and has acquired its own UAV for testing since this demonstration.

More recently, our team was in contact with SOCCIT, who expressed interest in a demonstration of using UAVs for collecting crash scene reconstruction imagery. Sgt. Craig Shackleford of the Bloomfield Township police and Angie Kremer of MDOT invited the project team to visit in early 2014. In April of 2014, MTRI team members traveled to the Bloomfield Township Police Department to an afternoon SOCCIT meeting where demonstration of UAVs was the main part of the agenda. Members of the Bloomfield Township, Troy, and Auburn Hills police attended, along with Michigan State Police personnel and other interested people.

Figure 6.2.3 A shows an example photo taken for that demonstration, with a second derived photo of an area near the police car. In them, the crash scene markers can be seen (small red and blue rectangles) that have been set up after a police vehicle laid down some tire marks. In the original 36 megapixel images, these could be used to measure distances because they were of a known size and were captured with high resolution. These markers were about 20x20 pixels per flat rectangular area, with a pixel equal to 1/11 inch (.0875 inches) or 0.22 centimeter

(2.2 millimeter). Figure 6.2.3 B shows 29 SOCCIT attendees viewing the UAV demonstration. The Bergen hexacopter, a DJI Phantom 1 with GoPro camera, and a DJI Phantom 2 were all shown. The small cameras flown with the DJI Phantoms were useful for quick, lower resolution imaging of the scene, while the Bergen hexacopter was paired with a larger Nikon D800 camera capable of the 36 megapixel resolution – this is more representative of what would be needed for crash scene measurements with sub-centimeter precision and accuracy.

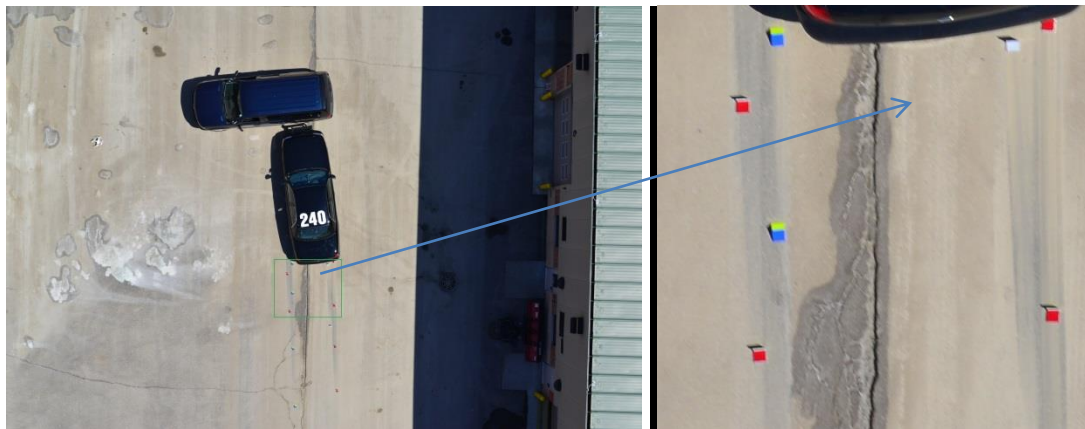


Figure 6.2.3 A: Example crash scene image hexacopter-based collection demonstration from April, 2014 for SOCCIT.



Figure 6.2.3 B: SOCCIT meeting attendees viewing the UAV demonstration for crash scene reconstruction imagery.

As shown above in the ITS World Congress (Section 4.4), an in-depth demonstration of UAVs to collect imagery for an emergency response mock incident was completed, including high-resolution images from the hexacopter / Nikon D800 combination and near real-time video from the traffic monitoring blimp. Figure 6.2.3 C is another example of the imagery that was able to be taken and then was able to be shared as soon as the hexacopter landed; providing high-resolution images during flight is a potential research area.

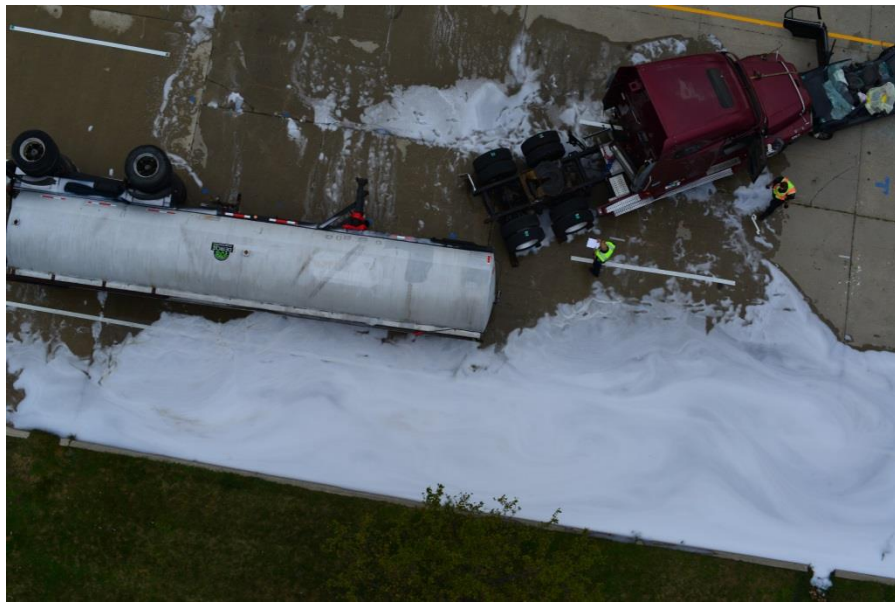


Figure 6.2.3 C: Additional crash scene image collected by the hexacopter-based system at the ITS World Congress.

We would expand from these efforts to complete a more formal demonstration and assessment of using UAVs for crash scene reconstruction documentation. Sgt. Shackleford, who saw both the SOCCIT and ITS World Congress demonstrations, appears eager to continue this as an applied research area. He offered to put the project team in contact with the Michigan Association of Traffic Accident Investigators (MATAI) as a potential partner for a larger demonstration. He also asked if the project team could accompany SOCCIT members on actual crash scene reconstruction events. For this additional task deliverable, we would:

- Complete two to three demonstrations for interested police agencies on using UAVs for crash scene reconstruction imaging.
- Accompany one or more police agencies on two to three actual crash scene reconstruction events.
- Work closely with Angie Kremer of MDOT, Sgt. Shackleford of SOCCIT, the program manager, and other appropriate people to develop this area into applied usage of UAVs, including understanding of the approval process for using UAVs.

- Produce a report describing the task results, concentrating on practical implementation by public safety agencies and focusing on a guidance document that provides practical implementation for public agencies.

6.2.4 A Demonstration of Slope Stability Assessment (for example, for retaining walls).

In a USDOT-funded project entitled “Sustainable Geotechnical Asset Management along Transportation Infrastructure Environment using Remote Sensing”

(<http://www.mtri.org/geoasset>), C. Brooks, T. Oommen (USDOT PI), and other team members have been evaluating and demonstrating a variety of technologies for measuring movement in unstable slopes and retaining walls. Some of these methods are UAV-based, others are vehicle-based, and some are satellite imagery-based. We would work with MDOT to select one or more sites where UAV-based assessment of slope or retaining wall movement would be appropriate, and document our results. In particular, a site with known retaining wall movement along M-10 in Southfield, MI near Meyers Road and McNichols Road (see Figure 6.2.4 A) has been monitored using ground-based optical photogrammetry methods, and results have shown promise. We would like to expand this test to an area more appropriate for UAV-based monitoring. In the team’s work in Alaska and Nevada, slopes near railroads and roadways are being monitoring for movement and are more suitable for evaluation than the urban “sunken freeway” retaining wall area along M-10. If a site can be selected where UAV-based assessment is practical for retaining walls, then these could be included as well.

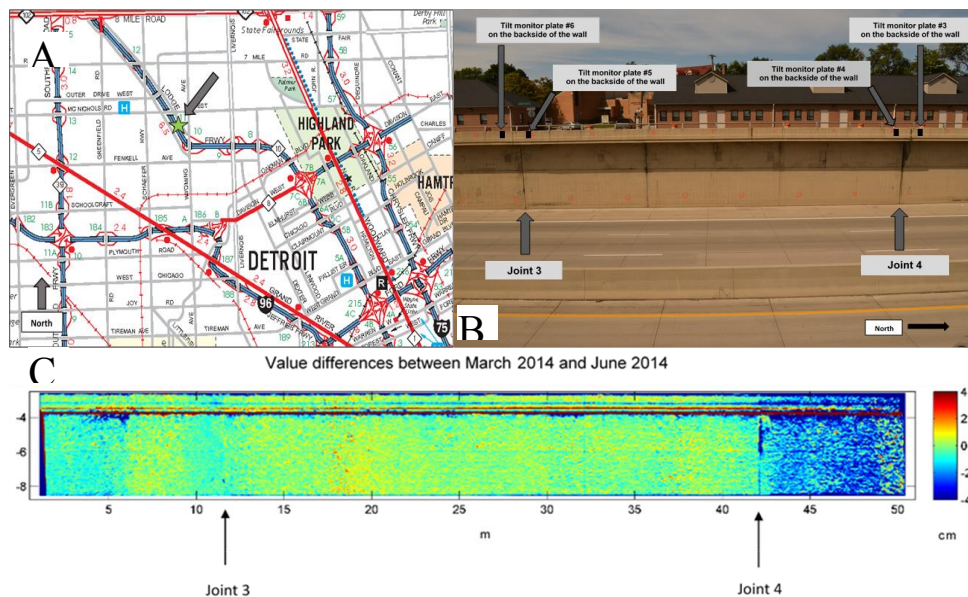


Figure 6.2.4 A) Location of Meyers site on M-10 highway northwest of downtown Detroit. **B)** Retaining wall section at Meyers site on M-10 highway. **C)** 3-D point cloud change detection showing movement in the wall panel starting at joint 4.

For this additional task deliverable, we would:

- Select two or three sites where UAV-based assessment of slope and retaining wall stability would be practical and valuable.
- Monitor these sites at least twice over the extended project period, creating 3-D models and tracking their movement over that time.
- Develop a report focusing on a guidance document that provides practical implementation for public agencies that describes where and how UAV-based slope stability assessment can be accomplished on a practical basis.

6.2.5 A Demonstration of the Capabilities to Complete Aerial Imaging to Meet MDOT Mapping and Construction Monitoring Needs

Our team has met with members of MDOT's Survey Support team, including John Lobbestael, Frank Boston, and Kelvin Wixtrom, who have expressed interest in better understanding the capabilities of UAVs and related image processing software for helping with their mapping needs. For this new deliverable task, the Michigan Tech project team would work closely with these staff to demonstrate how UAVs can meet their needs in a cost-efficient manner that increases safety and reduces data collection time. Examples that have been discussed include monitoring construction progress, volumetric calculations of aggregate (and other road/bridge construction resources), creating 3-D models of bridge elements such as pier bearings, and photogrammetric-quality imaging of priority MDOT sites. Figure 6.2.5 A is an example of a soil and gravel pile at a Michigan quarry that is currently being assessed for volumetric size for Dr. Oommen's Geotechnical Asset Management project. Figure 6.2.5 B is another example of a UAV-based image showing the "I-96 Fix" site in Livonia during construction in the summer of 2014. Figure 6.2.5 C is a close-up photo of a bridge bearing that would not have been possible without a bucket truck being available; instead, a small UAV was able to collect this image within a minute of being launched. Figure 6.2.5 D is an example where over 140 images taken from the hexacopter UAV were automatically stitched together into a single orthophotograph using image processing software as part of creating a high-resolution 3-D model of a bridge deck for automated spall detection.



Figure 6.2.5 A: Overhead photo of a soil and gravel pile at a Michigan quarry that can be used to help estimate volumetric content of the pile and its change over time.



Figure 6.2.5 B: The I-96 Fix major MDOT road and bridge rehabilitation project in Livonia, MI as viewed during construction when the Interstate was closed to traffic.



Figure 6.2.5 C: Close-up photo of bridge bearings, a beam, and the top of a pier cap taken with a small DJI Phantom UAV that would have needed a bucket truck to take the equivalent image.



Figure 6.2.5 D: Example of automatically stitching together over 140 images taken with the hexacopter UAV to create a single 2.5 millimeter resolution orthophoto of a bridge deck with significant condition problems such as spalling.

The project team would build from these discussions to complete a series of demonstrations that would enable the MDOT Survey Support team to better understand how UAVs could help them with their imaging and assessment needs on a practical basis. The project team anticipates demonstrations at two or more additional bridges, some stretches of highway, construction sites, and areas of interest to MDOT. Included as a result of these demonstrations would be a report recommended how MDOT could implement these capabilities to meet Survey Support and related needs, including sections on new FAA rules, options for in-house

data collection vs. UAV-based imaging as a third-party service, and the resolution capabilities of the demonstrated systems.

For this additional task deliverable, we would:

- Demonstrate practical UAV capabilities that can meet MDOT Survey Support imaging needs at three or more sites such as bridges, highways, and construction sites.
- Share data with MDOT Survey Support so they can understand and inspect the results themselves.
- Create a report focusing on a guidance document that provides practical implementation for public agencies documenting demonstration results, impacts of new FAA rules on implementation, data collection service options (in house vs. third-party), and the resolutions reached with the demonstrated systems.

6.2.6 A Report that Describes and Recommends Optimal Methods to Store and Distribute Potentially Large Imaging and 3-D Surface Datasets Created Through UAV-based Data Collection

Our research project is helping understand how these rapidly advancing imaging platforms can help achieve efficiencies in operations, maintenance, and asset management. However, the size of the generated data sets can be beyond what MDOT is used to currently managing for many of its programs, and there needs to be a way to handle the storage and distribution of these data. For this deliverable, we would work with MDOT staff, including those using GIS, to define and recommend how these raster and vector 2-D and 3-D geospatial data sets could most efficiently be stored, accessed, and visualized. Our recommendations would be delivered in a report co-authored with MDOT; MDOT Survey Support staff such as John Lobbestael have already expressed interest in helping with this evaluation as they anticipate receiving large data sets from UAV platforms in the near future.

The report would build from the data sets collected for bridge condition assessment, construction site imaging, traffic monitoring, confined space inspection, and LiDAR infrastructure collections. For example, for the Stark Road (I-96, Livonia) 3-D model and bridge condition assessment, the sizes of the data layers were:

- 140 input 36 megapixel images = 2.2 gigabytes total (see Figure 6.2.6 A for an example of one of these images)
- 3-D software processing project in Agisoft Photoscan = 600 megabytes
- Output orthophoto = 624 megabytes
- Output digital elevation model (DEM) = 236 megabytes
- Output detected spalls layer = 1 megabytes

This gives a total bridge deck assessment data set size of 3.7 gigabytes for a bridge with a deck area of approximately 180 feet long by 50 feet wide. Note that of these data sets, only the last three layers (orthophoto, DEM, and spalls layer) would need to be kept long term and available for GIS users and others wanting access to the UAV imaging processed results, or 0.86 gigabyte (861 megabytes).

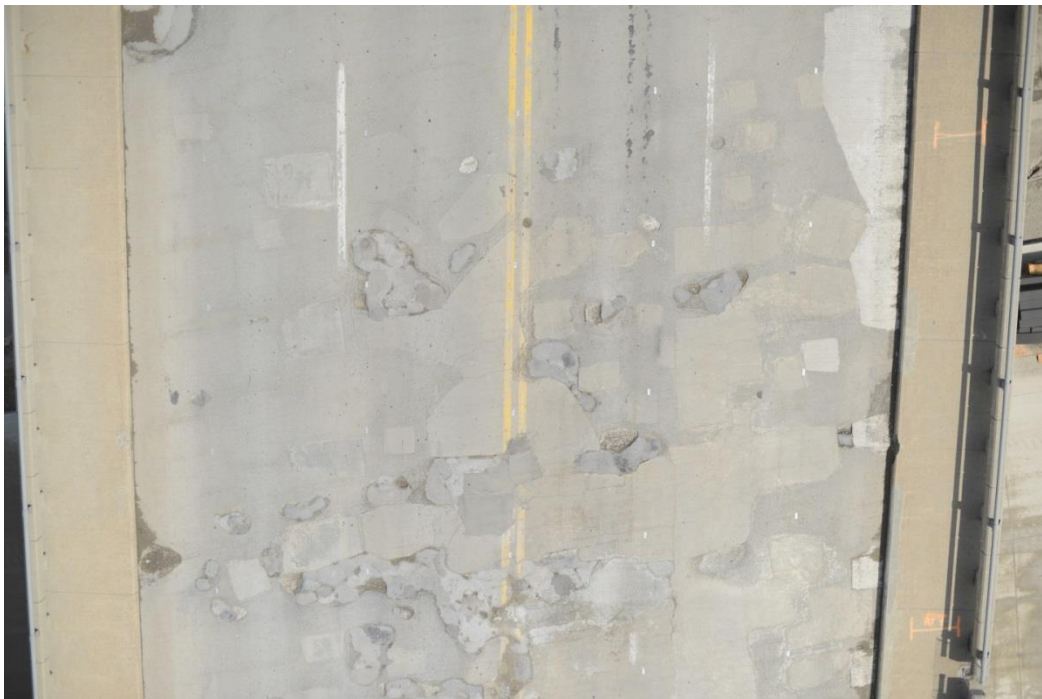


Figure 6.2.6 A: A single 36 megapixel (resolution), 16 megabyte (file size) image taken of the Stark Road bridge deck. About 140 of these were needed to create the 3-D model of the bridge deck, all collected with three minutes of flight time.

File storage space is an important issue, but data access methods are also important. It may be impractical for MDOT to make a 624 megabyte orthophoto available for users on its network, particularly with regional users. Technologies exist to make large images “streamable” over the Internet using image streaming web services. For a recent US Fish and Wildlife Service project, PI Brooks led an effort to evaluate four different web server technologies for making large raster datasets rapidly available to end users with image streaming technology; these software platforms were: ArcGIS for Server (v. 10.1), ERDAS Apollo Essentials 13.0 from Integraph (now Hexagon), Geoserver 2.2, and MapServer 6.2.0. Each of the platforms had strengths and advantages; ERDAS Apollo was fast, ArcGIS Server was easy to work with if you knew ESRI software already, GeoServer was free and easy to set up, and MapServer was free with speeds similar to ERDAS Apollo but needed more advanced configuration. The project team would build from these evaluations, and current MDOT and DTMB software plans, to recommend a

software platform or combination of software tools that could enable MDOT to access UAV-derived data sets quickly and cost-effectively.

Under this additional task deliverable, we would:

- Test software platforms to enable rapid and cost-effective access to potentially large data sets derived from UAV-based imaging.
- Co-author a report with MDOT focusing on a guidance document that provides practical implementation for public agencies based on testing, defining, and recommending how these 2-D and 3-D geospatial data sets could most efficiently be stored, accessed, and visualized

6.2.7 Enhanced Testing of UAV-based Thermal Imaging – Bridge Structural Integrity, Geotechnical Assets

Thomas Oommen and Theresa Ahlborn, Michigan Technological University

Ongoing research on the use of thermal cameras on a UAV based platform for transportation applications have explored their utility for examination of the structural integrity of bridge elements as part of the current MDOT UAV project. The focus of this effort has been to confirm technologies and define the system specifications, integration of hardware and software, and selection of site for field deployment. The testing of the technology was done using a Tau2 FLIR® camera with a 336 x 254 sensor array.

Current laboratory tests of known delaminations show that Tau2 FLIR® camera with a 336 x 254 sensor array can be promising to detect delaminations on bridge elements, at depths of 1, 1 ½, and 2 inches during periods of rapid temperature change as shown in Figure 6.2.7 A.

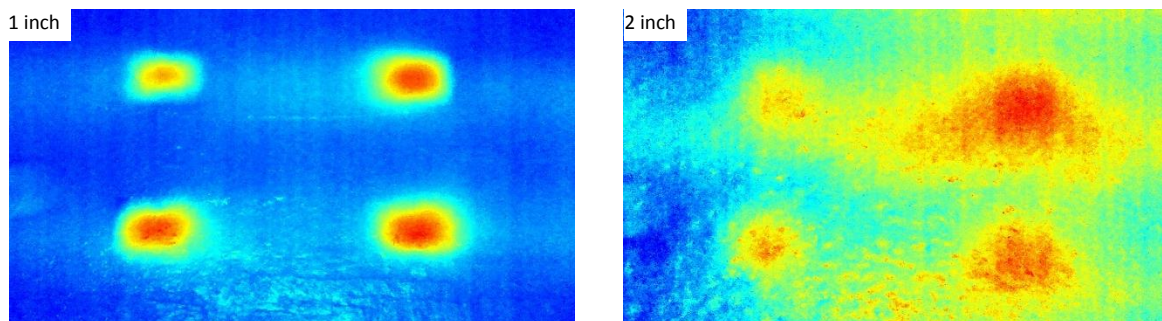


Figure 6.2.7 A: Thermal images captured after 30 minutes of heating with the 336 x 254 sensor array camera, showing delaminations in concrete slabs at 1 and 2 inches depth. Blue colors are lower temperature while yellow to red colors correspond to increasing temperatures. The higher temperature corresponds to locations with known delamination.

Figure 6.2.7 A shows that the size of delamination identified is better defined when the delamination is at a depth of 1 inch compared to the delamination at 2 inch depth. We plan to

test and improve this using a higher-resolution 640 x 512 sensor array Tau2 FLIR® camera. A comparison of the improved sensor capability is presented in Figure 6.2.7 B.

The current thermal sensor (336 x 254) resolution (pixel size on the ground) depends on the distance to the target and the lens optics (currently a 13 millimeter lens); for a UAV flying at 10 meters above the ground the resolution will be on the order of ~ 1 centimeter, giving a total field of view with a few meters width. The 640 x 512 sensor array Tau2 camera with the same 13 millimeter lens would allow to either double the size of the field of view maintaining the same resolution (by doubling the flight height above the ground), or double the pixel resolution (~ 0.5 centimeter). The higher resolution sensor will allow better quantification of the integrity of structural elements, exploring the limitations of resolution on different applications (e. g. on delamination detection), and compare and contrast the cost vs. benefit of the two systems. For instance, high frequency pixel noise and other problems would be minimized with a higher resolution sensor (e. g. the 640 x 512 sensor array).

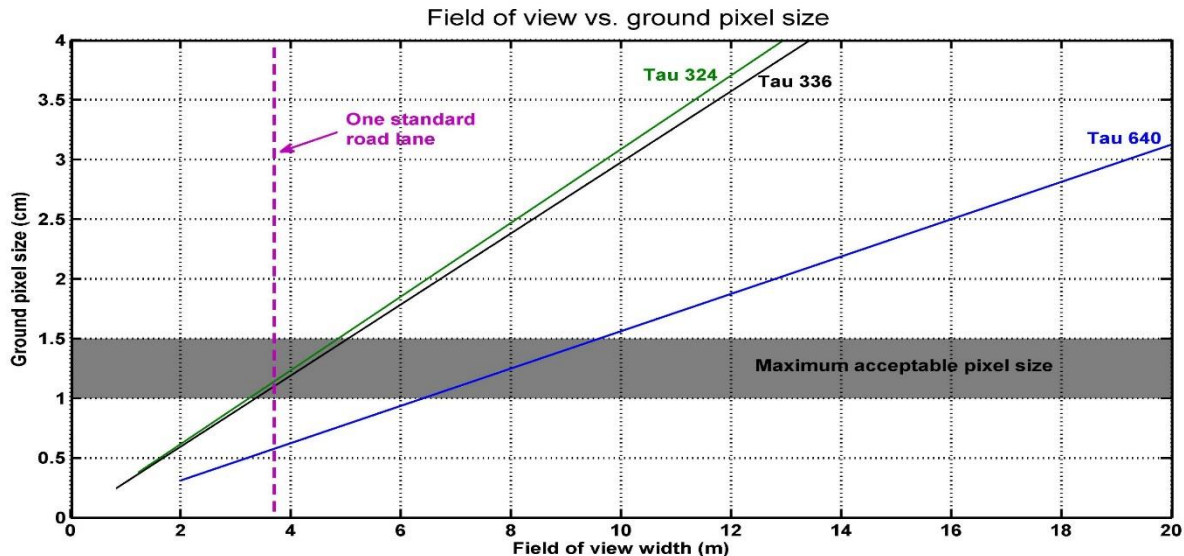


Figure 6.2.7 B: Comparison of the Tau 336 x 254 and Tau 640 x 512 sensors based on ground pixel size and field of view.

In addition, the proposed extension will verify the applicability of a UAV based thermal sensor for other transportation applications. Particularly, we will explore the applicability of thermal sensors in monitoring geotechnical assets (for example cut slopes, embankments, and retaining walls). Often the failure of geotechnical asset is controlled by structural weakness and/or the influence of ground water. The thermal sensors are valuable for monitoring the changes in ground water due to the inverse relationship of water content to temperature measurements. This deliverable task could be closely tied to the slope stability assessment proposed task (Section 6.2.4) to test both technologies, if desired.

In summary, based on the research progress so far, we are recommending the following additional deliverable components would be added to our current research project with MDOT under this task:

- Development, testing, and demonstration of improved quantification of the structural integrity of bridge elements using Tau2 FLIR® with a 640 x 512 sensor array.
- Demonstration of the applicability of thermal sensor on a UAV platform for other transportation application such as geotechnical asset management.
- A report focusing on a guidance document that provides practical implementation for public agencies summarizing the results of obtained with the improved thermal sensor as demonstrated with UAV-based data collection on bridges or other transportation infrastructure of interest to MDOT.

6.2.8 High Accuracy Simultaneous Thermal/Video/LIDAR Measurement Using a High-fidelity Sensor-fused UAV Positioning Approach

Geo-registered multi-modal sensor data has shown to be very useful in many remote sensing applications; e.g., agriculture, environmental monitoring, and transportation inspection. We aim to further the development of highly accurate methods for producing geo-registered, sensor-fused three-dimensional data of transportation infrastructure using UAV-based combined visible-spectrum video, thermal video, LIDAR, and inertial and spatial sensors. These data will enable research and development into using multi-sensor data for transportation purposes, such as inspection, inventory management, and maintenance trending. Furthermore, since the data will all be geo-registered, change detection and trending analysis will be enabled, allowing detection and measurement of temporal events such as bridge sagging, road bed changes, crack and spall migration, and missing roadway assets. A block diagram of the proposed process is illustrated in Figure 6.2.8 A. This objective encompasses four main tasks:

1. Investigate UAV-appropriate high quality positioning sensors, such as DGPS, GLONASS, base-station tracking, and digital terrain elevation data (DTED) maps;
2. Development of a generalized on-board computation platform that can simultaneously log multi-modal sensor data, such as visible and thermal video, LIDAR, hyperspectral imagery, and position sensors;
3. Development of a Simultaneous Location and Modeling (SLAM) algorithm that uses all available sensor data to accurately produce 3-D natural color and thermal imagery in a geo-registered coordinate system.
4. Demonstrate UAV-based multi-sensor analytics for transportation use case.

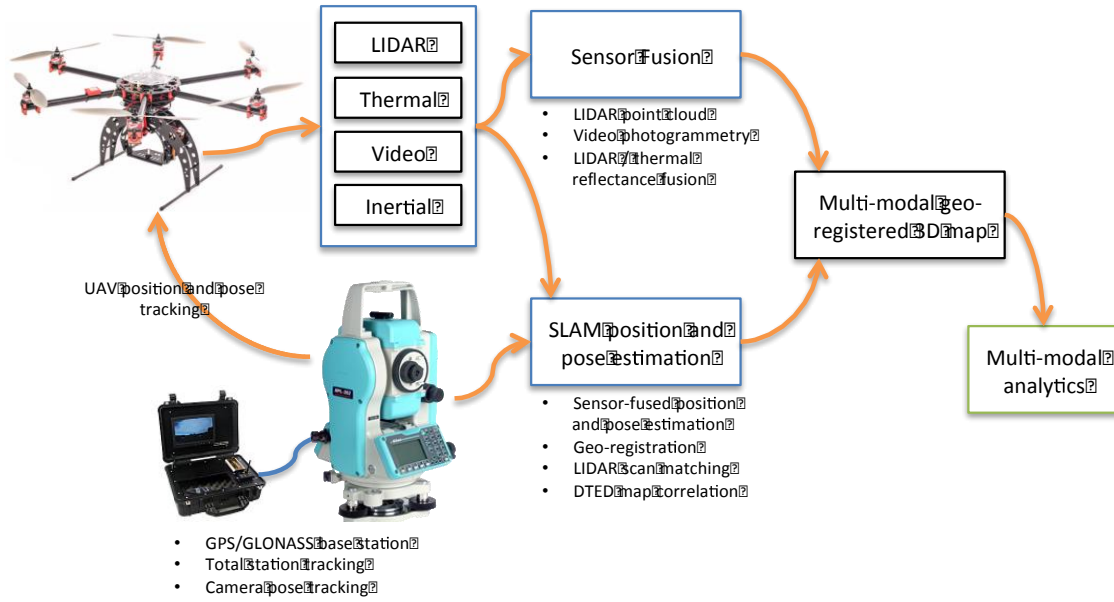


Figure 6.2.8 A: Block diagram of high accuracy UAV-based simultaneous thermal/video/LIDAR measurement and fusion.

One of the main challenges in using UAVs for remote sensing is that the location and pose of the vehicle at each sensor measurement is difficult to measure both in accuracy and precision. We have made significant strides in developing UAV-based LiDAR sensor pods and three-dimensional SLAM algorithms for the resulting measurements. Our algorithms currently use both LiDAR and inertial sensors to determine the position and pose of the vehicle, allowing us to combine multiple laser scans into a single point cloud. Preliminary results are very promising; see Figures 4.1.1 K and Figures 4.1.1 L, and Figure 6.2.86 B below. The main weakness in these results is that they are difficult to accurately geo-register, i.e., place in a global coordinate system such as (latitude, longitude, altitude) or UTM coordinates. Furthermore, certain assumptions are made about the measurement surface, which may be false. For example, to reconstruct the Merriman Rd. Bridge we assumed that the bridge was relatively flat across its span. While this is sufficient for showing local defects such as potholes/spalls or depressions, this assumption would be poor if the 3-D point cloud was used to look at overall bridge sag and declination. To combat this global accuracy problem, we would investigate higher quality position and altitude estimation using the fusion of two different approaches: i) geo-registration of the UAV flight using higher quality position sensing, such as differential GPS, GNSS, base station tracking, and digital terrain elevation data (DTED) maps; and ii) sensor-fused LiDAR plus video SLAM methods. Both these avenues of research will enable a much more accurate position and pose estimate of the UAV as it collects data, improving accuracy of data collections. Furthermore, simultaneous capturing of sensor data allows multi-modal analysis, which could be very important for highly accurate inspection and evaluation efforts.

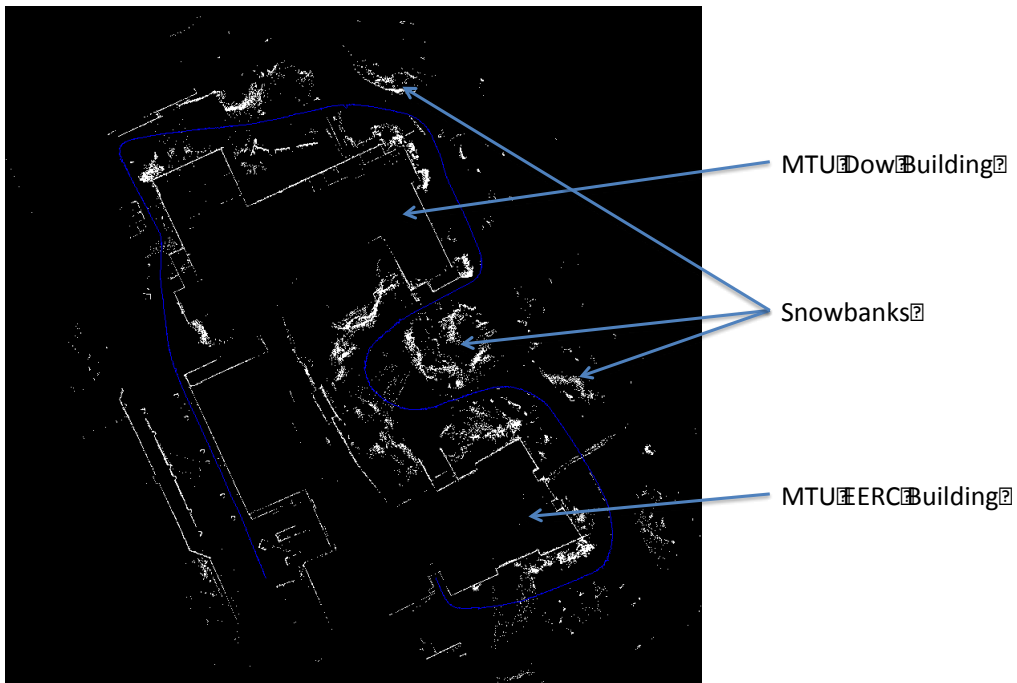


Figure 6.2.8 B: Three-dimensional scan of the MTU EERC and Dow buildings and surrounding areas.

Our first efforts will be on developing a on-board computational platform that can simultaneously synchronize and log sensor measurements from multiple sensors, e.g., thermal, video, and LIDAR. This computational platform will use the Nvidia Jetson embedded system that we currently use for this project. Further research will be necessary to investigate how to synchronize and time-stamp the multi-modal sensor observations.

Next, we will investigate the development of a base station approach for measuring the location of the UAV vehicle in the air. We will use a surveying total station to autonomously track a retro-reflector on the UAV. This will give a highly accurate position estimate relative to the base station (which can easily be geo-registered using commonly used surveying approaches and GPS averaging). To get a better measurement of the UAV pose (roll, pitch, and yaw), we will develop a autonomous computer vision approach that uses a camera at the base station to track multiple reflective markers on the UAV. Similar to methods used in motion capture for film, we can extrapolate the pose of the vehicle by inverting the location of the markers in the camera video.

We will fuse high-resolution visible and thermal imagery with the LIDAR data to create a three-dimensional image, where each point in the point cloud is colored according to the video imagery. Not only will this solve the geo-registration problem, but we also hypothesize that this additional position information will allow us to reduce the overall error in the point cloud measurement.

In summary, the end products and deliverables will be:

- A geo-registered three-dimensional natural color and thermal model of the sensed scene.
- A demonstration of using the multi-modal data for analytics in a transportation use case, such as a bridge inspection, road side asset inventory and assessment, or temporal trending analysis.
- A report focusing on a guidance document that provides practical implementation for public agencies describing the benefits of improved UAV positioning from multi-source, sensor-focused data for evaluating transportation infrastructure.

7. Conclusions and Recommendations

This applied research project enabled the testing and demonstration of five main UAV platforms, three types of sensors, four main types of infrastructure needs, extensive lab testing, and four main sets of demonstration. Presentations were made to the ITS World Congress and the Michigan Transportation Management Conference to enable local, regional, and international exposure to the results funded by MDOT research. Useful data were collected by one or more UAVs and a traffic monitoring blimp developed through the project, and this information was shared with MDOT through meetings, graphics, and other frequent communication. These data showed bridge deck surface and subsurface condition issues using UAV-collected imagery, how a construction or other priority site could be quickly imaged, rapid imaging of the underside of a bridge even when over water, and how small and “micro” UAVs could help evaluate if a confined space was safe to enter, including MDOT pump stations around the Detroit region. Improvements to the collection, processing, and visualization of data were enabled through the project. Project work improved the locations of LiDAR point cloud data and the use of lower-cost thermal sensor for mapping and quantifying subsurface bridge delaminations.

Together, these research efforts have shown that UAVs can help with many transportation issues, including providing flexible low-cost traffic monitoring, helping with needed bridge element inspection data including identifying spalls with optical images and likely delaminations with thermal data, evaluating the status and safety of confined spaces, and identifying types of “roadway assets” through UAV-based image analysis. Included as part of this report in section 6, as a second part of the Implementation Action Plan, are seven main ideas for potential further deliverable research tasks; these are focused on taking this project’s work towards implementation by MDOT on a practical basis. These recommendations for further research have previously been described, and are: 1) more formal crash scene imaging, 2) slope stability assessment, 3) aerial imaging to meet MDOT Survey Support and related needs, 4) optimal methods to store and share large UAV-based data sets, 5) improvements to UAV-based thermal imaging, 6) multi-sensor high-accuracy UAV positioning, and 7) traffic monitoring for a TOC.

The IAP describes the UAV technology demonstrations that are closest to near-term usage by MDOT, with a focus on bridge condition assessment, confined space inspection, and traffic monitoring. These match closely with the above potential further research ideas, which also include other MDOT priorities for further development and potential implementation. The project team recommends that MDOT select its highest priorities, within available funding limits, and chooses two or more of them to move forward with over the next year. Those that are not able to be advanced during the next year could become future research priorities starting in the 2015-2016 MDOT research cycle. Included as part of these new areas would be

more formalized costs assessments, since project work has focused on technical capabilities so far, with a goal for cost-efficient implementation.

With new rules on small UAVs due out from the FAA in late 2014, and new rules on commercial operations of UAVs due out in late 2015, UAV-based sensing of transportation infrastructure will become significantly more practical on a day-to-day basis over the next 18 months. However, it should be noted that public agencies can already obtain formal authorization from the FAA for use of UAVs through a certification process. The project team has been sharing advice with MDOT on this possibility and would like to continue this process.

Unmanned aerial vehicles and sensors that they can carry are developing rapidly. As recently as the turn of the decade in 2010, the idea would not have seemed reasonable that costs could be in the range of \$3000 for a high-resolution 36 megapixel camera, \$5400 for a very capable hexacopter UAV, \$800 for a small quadcopter porting a small camera with live video capabilities, \$4500 for a miniaturized thermal sensor, \$7000 for a small LiDAR unit, or \$1500 for a demonstration traffic monitoring blimp with a new 4G-capable camera sending near-live video. Processing and analysis software costs are becoming reasonable. When the PI first investigated close-range photogrammetric processing software capable of turning overlapping UAV-taken photos into high-resolution 3-D models, the main commercial package was over \$40,000; now we use a combination of a \$3500 commercial package and open source software that we have adapted to common high-resolution image processing needs. Mid-level, affordable desktop computers (at least eight cores, at least 64 gigabytes RAM) are now capable of processing the large data sets that can be generated with UAV-based imagery. Costs that are dropping for processing software, UAV platforms, lightweight capable sensors, and suitable computer hardware, combined with pending new FAA rules and greater agency and public exposure to the very positive capabilities of UAVs have made this the right time for MDOT to invest in evaluating UAV capabilities to help with its transportation priorities. The project team thanks MDOT for the opportunity to demonstrate UAV capabilities and looks forward to moving the results to implementation.

8. References

- ACI (2001). Protection of Metals in Concrete against Corrosion (ACI 222R). Farmington Hills, MI, American Concrete Institute.
- Ahlborn, T. M., Shuchman, R., Brooks, C. N., Burns, J. W., Endsley, K. A., Evans, D. C., Vaghefi, K., Oats, R. C., & Harris, D. K. et al (2012). Bridge Condition Assessment Using Remote Sensors. Bridge monitoring using wireless smart sensors. SPIE Newsroom: SPIE.
- Ahlborn, T. M., R. Shuchman, L. L. Sutter, D. K. Harris, C. N. Brooks, and J. W. Burns (2013). Bridge condition assessment using remote sensors. Final project report, USDOT/RITA. Cooperative agreement # DTOS59-10-H-00001.
- Alqennah, H. (2000). Detection of subsurface anomalies in composite bridge decks using infrared thermography. Department of Civil and Environmental Engineering. Morgantown, WV, West Virginia University. Master of Science in Civil Engineering: 95.
- American Association of State Highway and Transportation Officials (AASHTO) (2008). Bridging the Gap: Restoring and Rebuilding the Nation's Bridges.
- ASTM (2007). ASTM D4788-03: Standard test method for detecting delaminations in bridge decks using infrared thermography, American Society of Testing Materials.
- Barazetti, L., F. Remondino, and M. Scaioni (2010). Automation in 3-D reconstruction: results on different kinds of close-range blocks. *Int. Arch. Photogramm., Remote Sens. Spat. Inf. Sci.*, 38, pp. 55-61.
- Bourgault, F. and H.F. Durrant-Whyte (2004). Communication in general decentralized filters and the coordinated search strategy. In *Proc. Int. Conf. Information Fusion*, pp. 723-730.
- Brooks, C., C. Roussi, T. Colling, D. Dean, and R. Dobson (2013). Characterization of Unpaved Road Conditions through the Use of Remote Sensing". TRB Presentation # P13-6289 at the Special Workshop on Sensing Technologies for Transportation, 2013 TRB Annual Conference, Washington, D.C.
- Chiabrando, F., F. Nex, D. Piatti, and F. Rinaudo (2011). UAV and RPV systems for photogrammetric surveys in archaeological areas: two tests in the Piedmont region (Italy). *J. Archaeol. Sci.*, 38, pp. 697-710.
- Choi, K., I. Lee, J. Hong, T. Oh, and S. Shin (2009). Developing a UAV-based rapid mapping system for emergency response. *Proc. SPIE*, 7332.
- Clark, R. N., Swayze, G. A., Livo, K. E., Kokaly, R. F., Sutley, S. J., Dalton, J. B., McDougal, R. R., and Gent, C. A., 2003. Imaging spectroscopy: earth and planetary remote sensing with

the USGS Tetracorder and expert systems. *Journal of Geophysical Research*, doi:10.1029/2002JE001847.

Croom, M.A., J.S. Levine, D.A. Spencer, R.D. Braun, and H.S. Wright (2004). The Mars airplane: a credible science platform. In *Proc. IEEE Aerospace Conference*.

Dandoi, J.P. and E.C. Ellis (2010). Remote sensing of vegetation structure using computer vision. *Remote Sens.*, 2, pp. 1157-1176.

DARLA: Data Assimilation and Remote Sensing for Littoral Applications.

<http://www.apl.washington.edu/project/project.php?id=darla>

Del Grande, N.K., P. F. Durbin, C. M. Logan, D. E. Perkins, P.C. Schaich (1996). Demonstration of dual-band infrared thermal imaging at Grass Valley Creek Bridges, in Proceedings of SPIE Conference 2944: Nondestructive Evaluation of Bridges and Highways, Ed. S. Chase, Scottsdale, AZ, pp. 166-177, Dec. 1996.

Fawcett, T. (2006). An Introduction to ROC Analysis. *Pattern Recognition Letters* 27(8): 861-874.

Henriksen, S. (Editor) (1994). The Glossary of the Mapping Sciences. American Society of Civil Engineers, New York, NY, American Society for Photogrammetry and Remote Sensing and American Congress on Surveying and Mapping, Bethesda, MD.

Hunt Jr., E., W. Hively, S. Fijukawa, D. Linden, C. Daughtry, and G. McCarty (2010). Acquisition of NIR-green-blue digital photographs from unmanned aircraft for crop monitoring. *Remote Sens.*, 2, pp. 290-305.

Jaakkola, A., J. Hyypa, A. Kukko, X. Yu, H. Kaartinen, M. Lehtomaki, and Y. Lin (2010). A low-cost multi-sensoral mobile mapping system and its feasibility for tree measurements. *ISPRS J. Photogramm.*, 65, pp. 514-522.

Jenson, J. (2007). Remote sensing of the environment: an earth resource perspective, Pearson Education, Inc.

Jiang, R., D. V. Ja'uregui, K. R. White (2008). Close-range Photogrammetry Applications in Bridge Measurement: Literature review. *Measurement*, 41(8): 823-834.

Jiang, W., F. Wenkai, and L. Qianru (2013). An integrated measure and location method based on airborne 2-D laser scanning sensor for UAV power line inspection. In *Proc. Int. Conf. Measuring Tech. and Mechatronics Automation*, pp. 213-217.

- Jutzi, B., M. Weinmann, and J. Meidow (2013). Improved UAV-borne 3-D mapping by fusing optical and laserscanner data. *Int. Arch. Photogrammetry, Remote Sensing, and Spatial Info. Sci.*, XL-1/W2, pp. 223-228.
- Kim, J.H., M. Ridley, A. Goktogan, H. Durrant-Whyte, S. Sukkarieh, and E. Nettleton (2003). The ANSER Project: data fusion across multiple uninhabited air vehicles. *Int J. Robotics Research*, 22(7), pp. 505-539.
- Laliberte, A.S., M.A. Goforth, C.M. Steele, and A. Rango (2011). Multispectral remote sensing from unmanned aircraft: image processing workflows and applications for rangeland environments. *Remote Sens.*, 3, pp. 2529-2551.
- Landers, M.N. (1992). Bridge scour data management: Proceedings of Environmental Engineering Sessions Water Forum, American Society of Civil Engineers, p. 1094 – 1099.
- Lin, Y., J. Hyppa, and A. Jaakkola (2011). A mini-UAV-borne LIDAR for fine-scale mapping. *IEEE Geosci. Remote. Sens.*, 8, pp. 426-430.
- Lin, Y. and S. Saripalli (2012). Road detection and tracking from aerial desert imagery. *J. Intelligent and Robotic Sys.*, 65(1-4), pp. 345-359.
- Loubere, P. (2012). The Global Climate System. *Nature Education Knowledge* 3(10): 24.
- Luhmann, T., S. Robson, et al. (2007). Close range photogrammetry: principles, techniques and applications, Wiley.
- Maas, H. and U.Hampel (2006). Photogrammetric technique in civil engineering material testing and structure monitoring. *Photogrammetric Engineering & Remote Sensing* 72, 1-7.
- Maldague, X. P. V. (1993). Nondestructive evaluation of materials by infrared thermography. London, Springer-Verlag.
- Maser, K. R. and W. M. K. Roddis (1990). Principles of thermography and radar for bridge deck assessment. *Journal of Transportation Engineering*, 116(5): 583-601.
- McGlone, J.C., E.M. Mikhail, J.S. Bethel, and R. Mullen (Editors) (2004). Manual of Photogrammetry, Fifth Edition. American Society for Photogrammetry and Remote Sensing, Bethesda, MD..
- Merino, L., F. Caballero, J. R. Martinez-de-Dios, I. Maza, and A. Ollero (2012). An unmanned aircraft system for automatic forest fire monitoring and measurement. *J. Intelligent and Robotic Sys.*, 65(1-4), pp. 533-548.

- Miller, R. and O. Amidi (1998). 3-D site mapping with the CMU autonomous helicopter. In *Proc. Int. Conf. Int. Auto. Syst.*
- Nagai, M., R. Shibasaki, H. Kimagai, and A. Ahmed (2009). UAV-borne 3-D mapping system by multisensory integration. *IEEE Trans. Geosci. Remote Sens.,* 47, pp. 701-708.
- Pohl, C. and J.L. Van Genderen (1998). Multisensor image fusion in remote sensing: concepts, methods and applications. *Int. J. Remote Sensing* 19(5), 823-854.
- Rogers, K.J. (2013). Frequency estimation for 3-D atmospheric tomography using unmanned aerial vehicles. In *Proc. IEEE Int. Conf. Int. Sens., Sens. Nets., and Info. Proc.,* pp. 390-395.
- Russ, M., M. Vohla, and P. Stutz (2012). LIDAR-based object detection on small UAV: integration, experimentation, and results. In *Proc. Infotech@Aerospace,* pp. 1-6.
- Serrano, N.E. (2011). Autonomous quadrotor unmanned aerial vehicle for culvert inspection. M.Eng. Thesis, MIT.
- Starnes, M. A. (2002). Development of technical bases for using infrared thermography for nondestructive evaluation of fiber reinforced polymer composites bonded to concrete. Civil and Environmental Engineering, Massachusetts Institute of Technology.
- Sugiura, R., N. Noguchi, and K. Ishii (2005). Remote-sensing technology for vegetation monitoring using an unmanned helicopter. *Biosyst. Eng.,* 90, pp. 369-379.
- Tao, W., Y. Lei, and P. Mooney (2011). Dense point cloud extraction from UAV captured images in forest area. In *Proc. IEEE Int. Conf. Spat. Data Mining and Geo. Know. Serv.,* pp. 398-392.
- Triggs, B., P. F. McLauchlan, R. I. Hartley, and A. L. Fitzgibbon. (2000) Bundle Adjustment - A Modern Synthesis. Vision Algorithms '99. LNCS 1883. pp. 298-372.
- US Department of Transportation Research and Innovative Technology Administration (US DOT RITA) (2012). Development of UAV-based remote sensing capabilities for highway applications. University Transportation Center Spotlight.
- Vaghefi, K., T. Ahlborn, D. Harris, and C. Brooks (2013). Combine imaging technologies for concrete bridge deck condition assessment. J. Performance of Constructed Facilities 10.1061.
- Wallace, L., A. Lucleer, C. Watson, and D. Turner (2012). Development of a UAV-LIDAR system with application to forest inventory. *Remote Sens.,* 4, pp. 1519-1543.

Washer, G., R. Fenwick, N. Bolleni (2009). Development of hand-held thermographic inspection technologies. OR10-007.

Wester-Ebbinghouse, W. (1988). Analytics in non-topographic photogrammetry. ISPRS Cong., V., Kyoto 27(B11), 380-390.

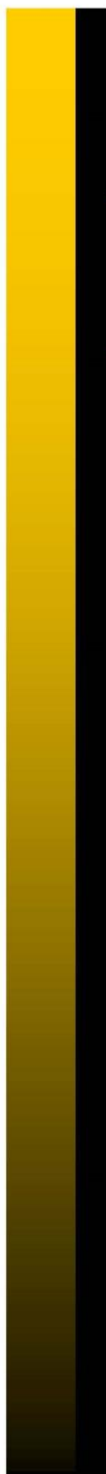
Zhang, H., Y. Lan, C.P. Shu, J. Westbrooks, W.C. Hoffmann, C. Yang, and Y. Huang (2013). Fusion of remotely sensed data from airborne and ground-based sensors to enhance detection of cotton plants. Computers and Electronics in Agriculture 93, 55-59.

9. Appendices

9.1 List of Acronyms, Abbreviations and Symbols

2-D	Two Dimensional
3-D	Three Dimensional
3DOBS	3-D Optical Bridge-evaluation System
ARF	Almost Ready to Fly
AUC	Area Under the Curve
BRISK	Binary Robust Invariant Scalable Keypoints
CCD	Charge Coupled Devices
CSV	Comma Separated Values
DEM	Digital Elevation Model
DSLR	Digital Single Lens Reflex
DTED	Digital Terrain Elevation Data
FAA	Federal Aviation Administration
FLIR	Forward Looking Infrared
FOV	Field of View
FPS	Frames per Second
FPV	First Person Viewer
GNSS	Global Navigation Satellite System
GPS	Global Positioning System
HD	High Definition
IAP	Implementation Action Plan
IMU	Inertial Measurement
INS	Inertial Navigation Sensor
ITS	Intelligent Transportation System
IR	Infrared
JPG / JPEG	Joint Photographic Experts Group
KLT	Kanade-Lucas-Tomasi
LiDAR	Light Detection and Ranging
MATAI	Michigan Association of Traffic Accident Investigators
MDOT	Michigan Department of Transportation
MP	Megapixel
MSP	Michigan State Police
MTRI	Michigan Tech Research Institute
NDE	Non-Destructive Evaluation
NOTAM	Notice to Airmen
OS	Operating System
PBOS	Performance-Based Operational System
PDRP	Property Damage Reclamation Process
PI	Principal Investigator
PM	Program Manager
RCOC	Road Commission for Oakland County
RGB	Red, Green, Blue
RMS	Root Mean Square
ROC	Receiver Operating Characteristic
RTF	Ready to Fly
SEMTOC	Southeast Michigan Traffic Operation Center
SIFT	Scale-Invariant Feature Transform
SLAM	Simultaneous Location and Mapping
SOCCIT	Southeast Oakland County Crash Investigation Team
SURF	Speeded Up Robust Features
TAMS	Transportation Asset Management System
TIFF	Tagged Image File Format
TOC	Traffic Operation Center
UAV	Unmanned Aerial Vehicles
US DOT	United States Department of Transportation

9.2 State of the Practice for Remote Sensing of Transportation Infrastructure Using Unmanned Aerial Vehicles (UAV)



www.mtri.org

State of the Practice for Remote Sensing of Transportation Infrastructure Using Unmanned Aerial Vehicles (UAV)

**Colin Brooks, Richard J. Dobson, Thomas Oommen,
Timothy Havens, Theresa M. Ahlbom, Dave Dean, David
Banach, Nate Jessee, Rudiger Escobar Wolf - Michigan
Technological University**

October 31, 2013

Michigan Tech Research Institute (MTRI)
3600 Green Court, Suite 100 • Ann Arbor, Michigan 48105

Table of Contents

Table of Contents.....	i
I. Introduction.....	1
II. NDE techniques with remote sensors used for transportation-related assessment.....	2
2.1 Optical	2
2.2. Thermal.....	5
2.3. LiDAR.....	11
III. Applicable Platforms.....	17
3.1. Single Rotor Helicopters.....	17
3.2. Multi-rotor Helicopters.....	19
3.3. Fixed Wing	21
3.4. Blimp/ balloon/ aerostat.....	22
IV. Application of Remote Sensors on UAV Platforms	25
4.1. Confined Spaces	25
4.2. Traffic Monitoring.....	26
4.3. Infrastructure assessment.....	28
V. Current Use of UAVs for Transportation	33
VI. Conclusion	35
VII. References	36

I. Introduction

The use of Unmanned Aerial Vehicles (UAVs) as a stable platform for remote sensing has been the center of several studies, and practical applications for transportation are starting to come to the forefront with this rapidly developing technology. The purpose of this report is to review the types of sensors, platforms, and applications that reflect the current state of the practice in applying UAVs for remote sensing of transportation infrastructure and similar assessments. The focus is on lower-cost "small" UAV (less than 55 lbs) solutions that are of near-term value to the Michigan Department of Transportation, rather than more expensive solutions (>\$25k).

UAVs are also known as Unmanned Aerial Systems (UAS) and "drones" (a term not popular in the professional UAV community). They can be equipped with a variety of sensors, including optical (visible and near-infrared light), thermal, and LiDAR. They also come in several main platforms, including single-rotor helicopters, multi-rotor helicopters, tethered devices (such as balloons and blimps), and fixed-wing aircraft. The "small UAV" definition is based on pending regulations from the Federal Aviation Administration (FAA) supposed to be released in late 2013 where unmanned aircraft under 55 lbs (25kg) are defined as small. These regulations should be friendlier to more practical day-to-day operation than related regulations for larger commercially operated UAVs. Under the FAA Modernization and Reform Act of 2012, the FAA is required to issue regulations for commercial operation of UAVs in the National Airspace (NAS) by September 30, 2015. Currently, outdoor usage of non-tethered UAVs is fairly restricted (see http://www.faa.gov/about/initiatives/uas/uas_faq/) with operation restricted to public agencies (including public universities) that receive a Certificate of Authorization and to a small number of firms that have obtained experimental certificates for device testing.

What this means for transportation agencies is that they can investigate current and near-term applications, fly outdoors with appropriate permission, and prepare for the upcoming new regulatory world that will enable more frequent, easier use of UAVs within the next 2 years.

II. NDE techniques with remote sensors used for transportation-related assessment

2.1 Optical

Optical remote sensing is most commonly done by using sensors that are sensitive to the visible portion of the electromagnetic spectrum. This corresponds to wavelengths of light are between 400 and 700 nm. Optical systems are able to detect near infrared (IR) wavelengths of light (approximately 700 to 1300 nm or 1.3 microns) but use filters to prevent them from being detected by the sensor; however, digital cameras can have their filter removed. The most common optical sensors are Charge-Coupled Devices (CCDs), which are used in typical consumer-grade digital cameras. The wide scale availability of digital cameras and low cost make them a good candidate for characterizing remote sensing applications. These sensors have been developed to be smaller as they are used for cell phone cameras as well as in professional photography.

Optical-based UAVs have been successfully used to measure 3D point clouds, e.g., in archeological surveys (Barazzetti et al., 2010, Chiabrando et al., 2011), vegetation monitoring (Sugiura et al., 2005, Laliberte et al., 2011, Hunt et al., 2010), and forest monitoring (Tao et al., 2011, Dandois and Ellis, 2010).

For application on UAV platforms, there needs to be a balance between size of the sensor (i.e. weight) and resolution. High resolution DSLRs (Digital Single-Lens Reflex) cameras are able to capture imagery at over 20 Mega Pixels (MP) but that comes at the cost of weight. The Nikon D800 has a sensor that is 36.3 MP which is capable of producing high resolution (< 0.3 in) imagery while being flown at a distance of 100 ft from the target (Brooks et al. 2013). The disadvantage of this camera on a UAV platform is the size and weight. This camera can only be carried by larger UAVs as the camera and lens weigh about 2.5 lbs (Figure 1). These types of cameras are more suited to be used for capturing imagery of bridges and other road infrastructure. Newer very high resolution cameras are being released, though; Sony recently announced the 7R camera with a 36 MP sensor being released in December 2013, which weighs ½ lbs (407g without lens) and has the potential to be mounted on smaller UAVs. Some UAV vendors are also testing the capability of the Lumia 1020 cell phone that has a built-in 41 MP camera.



Figure 1. Example of a Nikon D800 mounted below a Bergen Tazer 800 single rotor UAV ready for deployment.

Smaller "point and shoot" cameras typically offer resolutions of up to 20 MP and are significantly smaller than DSLRs. An example is the Nikon Coolpix S4400 (Figure 2a) which has a resolution of 20.1 MP but only weighs 5 oz. These cameras are more often used on fixed wing UAVs because of their light weight and smaller profile. Another camera option would be GoPro cameras which were originally designed for recording extreme sports (Figure 2b). These cameras are capable of 12 MP imagery and only weigh 2.8 oz. These cameras are more suitable for smaller UAVs with their lower weight, but that comes with reduced resolution. The advantage of the GoPro is that it is capable of capturing higher frame rates than a typical point and shoot camera. While in video mode, the GoPro Hero 3 can take 4K CIN (8.8 MP per frame) video at 12 frames per second and 12 MP stills at 2 frames per second. The advantage of taking high frame rate imagery would be the ability to collect overlapping imagery from a UAV that is flying near or quickly past a feature of interest.



Figure 2. A Nikon Coolpix S4400 (left) which is capable of taking 20.1 MP pictures is a smaller lighter alternative to DSLRs. The GoPro Hero 3 (right) is smaller than a typical point and shoot camera that is capable of higher frame rates.

For the inspection of confined spaces, a smaller camera may be necessary depending on the lift capacity of the UAV used and the size of the confined space. Smaller cameras such as those found in cell phones are the smallest cameras that can be practically used. Figure 3 show a Crazyflie Nano quadcopter (3.5 in. across) with a keychain camera mounted to it. The camera is capable of taking 2MP HD video. The disadvantage is that flight time can be very limited (in the 2-4 minute range).



Figure 3. Crazyflie Nano (3.5 in across and weighs 0.67 oz) with a keychain camera mounted on top.

Aside from acquiring photo inventories or transmitting video of bridges, confined spaces, and other transportation infrastructure, the photos taken from a UAV can also be used to extract additional, three-dimensional information through photogrammetric techniques. Photogrammetry is “the science or art of deducing the physical dimensions of objects from measurements on photographs of the objects” (Henriksen 1994). This includes measurements made from both film and digital photography. Digital photogrammetry has been demonstrated as a viable technique for generating 3D models of structures and structural elements (Maas and Hampel 2006). In order to perform 3D photogrammetry, the photos need to be taken with at least a 60% overlap (McGlone et al. 2004). This ensures that a feature on the ground is represented in at least two photos, as illustrated in Figure 4. At the altitudes that most UAVs will operate this technique is more specifically called close-range photogrammetry. Close-range photogrammetry is defined as capturing imagery of an object or the ground from a range of less than 100 m (328 ft) (Jiang et al. 2008).

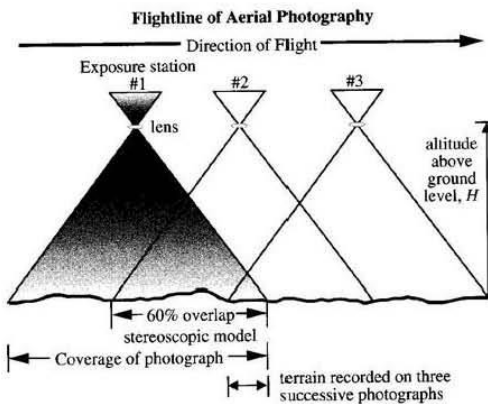


Figure 4. An example of how stereoscopic imagery for generating 3D models is collected (Jenson 2007).

Typically, 3D models are generated by using the bundle adjustment principle (Triggs et al. 2000). This process used determines the orientation of each image in a series of overlapping images to generate a sparse point cloud (Triggs et al 2000). Figure 5 shows the triangulation between multiple images that is used during this process. This process allows for images to be taken at different angles, which occurs when the camera rolls and changes pitch as it is moved across its target.

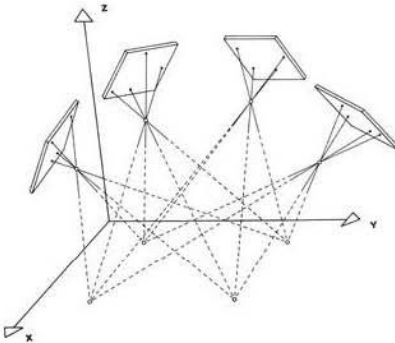


Figure 5. Bundle adjustment seeks to solve the geometry between photos and to generate 3D point clouds. This figure shows the relationship between four images that is solved by the bundle adjustment (Wester - Ebbinghaus 1988).

This technique allows for additional height information to be extracted from the imagery. Various distresses, such as spalls, cracking, and ruts can be detected and characterized by generating Digital Elevation Models (DEM) from this additional three-dimensional data. With recent advances in close range photogrammetric software, the generation of DEMs is mostly automated. Some software applications, such as Agisoft PhotoScan, only require the user to input the photos and a 3D model is generated without any further interaction. In order to generate a DEM the user has to set up a real-world projected coordinate system. This is done by placing markers with known GPS coordinates on the surface being modeled or by geo-tagging the images as they are taken. This technique was used by Ahlborn et al. (2013) to locate spalls on bridge decks with a truck-mounted camera and also by Brooks et al. (2013) to characterize distresses on an unpaved road.

2.2. Thermal

2.2.1. Basic concepts of thermal remote sensing monitoring

The basic concepts of thermal remote sensing presented in this section follow the general description given in standard textbooks on remote sensing (e.g., Jensen, 2007); for a more detailed explanation of these concepts the reader should consult such a text and the references therein. Thermal remote sensing is based on the physical process by which physical surfaces radiate electromagnetic energy as a function of their temperature. Thermal remote sensing instruments usually sense and record the radiance reaching the sensor after being emitted by a hot surface located at some distance from the instrument. The intensity and spectral content of the radiated energy depends not only on the surface temperature, but also on the material properties, especially the emissivity. The relationship between surface temperature and emitted electromagnetic energy can be described based on the concept of an ideal surface, known as a blackbody radiator, which absorbs all the incident radiation (there is no energy reflected) and only emits energy as a function of its temperature, according to Planck's law (see equation 1), as shown in Figure 6. The following formulates the relationship of surface temperature and emitted electromagnetic energy,

$$B_{\lambda}(T) = \frac{2hc^2}{\lambda^5} \left(\frac{hc}{e^{\lambda/k_B T} - 1} \right)$$

Equation 1.

Where B_{λ} is the spectral radiance given in Watts per m^2 per steradian (solid angle unit) per micrometer ($W m^{-2} sr^{-1} \mu m^{-1}$); h is the Planck constant ($6.62 \times 10^{-34} J s$); c is the speed of light in m/s ; λ is the wavelength of the radiation in m ; k_B is the Boltzmann constant ($1.38 \times 10^{-23} JK^{-1}$); and T is the temperature in Kelvin.

Real objects (sometimes called “gray bodies”) do not behave as ideal blackbody radiators and emit less electromagnetic energy than would be emitted by a blackbody at the same temperature; the ratio of energy emitted by a real surface to that emitted by an ideal blackbody radiator at the same temperature is called the emissivity; it is always a value between 0 and 1 (1 being the emissivity of a blackbody radiator), and is a property of each specific surface.

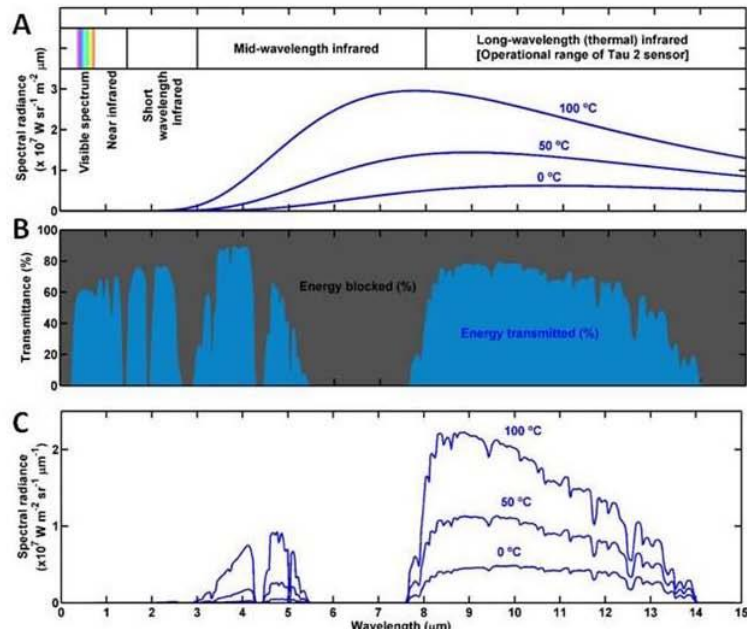


Figure 6. A Spectral radiance as a function of wavelength according to Planck's law. The three curves represent surfaces at different temperatures. The upper extreme of part A also shows the classification of different regions of the electromagnetic spectrum, including the long-wavelength or thermal infrared region, on which most thermal remote sensing instruments work, including the FLIR Tau 2 sensor discussed later. B Typical atmospheric transmittance through a whole vertical atmospheric column (adapted from Loubere, 2012) for the same wavelengths shown in panel A. Notice the “thermal window” between 8 and 14 μm coinciding with the thermal infrared part of the spectrum, and for which the atmospheric transmittance is high, allowing electromagnetic radiation to travel without much absorption. C Spectral radiance transmitted through the atmosphere considering the transmittance shown in panel B.

$$j = \sigma T^4$$

Equation 2.

Where j is the emissive power in Watts per m² (W m⁻²); σ is the Stefan-Boltzmann constant (5.67×10^{-8} W m⁻² K⁻⁴); and T is the temperature in Kelvin.

This law applies only to ideal blackbody radiators (emissivity = 1), and for real objects with an emissivity of less than 1, the actual emissive power will be less by a factor given by the emissivity. From this it follows that the real temperature will also depend on the emissivity according to

$$\varepsilon = \left(\frac{T_{brightness}}{T_{kinetic}} \right)^4 \quad \text{Equation 3.}$$

where ε is the emissivity (non-dimensional), $T_{brightness}$ is the temperature that would correspond to a blackbody surface emitting the observed radiance, and $T_{kinetic}$ is the real temperature of the surface.

For this reason, the emissivity of the surface becomes crucial in relating the temperature we want to measure to the radiance recorded by the remote sensing instrument. Emissivity values for opaque, dark colored materials tends to be high, i.e., close to 1 (e.g., $\varepsilon > 0.9$ for asphalt and rough concrete), whereas emissivity values for highly reflective surfaces can be very low, that is, close to 0 (e.g., $\varepsilon < 0.1$ for polished metallic surfaces).

In summary, it can be said that the sensors used in thermal remote sensing usually sense and record the radiance reaching the sensor, and therefore additional data processing is necessary to derive more commonly used physical quantities, like temperature or emissive power. The main variables to consider are related to the atmospheric absorption and the properties of the emitting surface, in particular its emissivity.

2.2.2. Thermal monitoring applied to concrete surfaces

Applications of thermal remote sensing to monitor concrete surfaces in the transportation environment are mainly aimed to detect anomalies associated to delaminations and similar structural defects (Maser and Roddis 1990; Washer et al. 2009 and 2010; ASTM 2007; and ACI 2001). Detection of such defects, e.g., delaminations, will enable infrastructure inspectors to identify damaged areas before delaminations develop into spalls (Ahlborn et al. 2012). The basic idea behind such an approach is that the concrete surface changes temperature due to changes in the environmental conditions, either due to natural variation, e.g., the diurnal temperature and insolation changes, or due to artificial heat sources, e.g., heaters deployed for testing purposes. The temperature changes differently affect areas with defects (e.g., delaminations) than they do intact areas, resulting in temperature differences that can be detected with the thermal remote sensing methods. The areas with defects can be inferred and mapped from the radiance or temperature differences, even if they would otherwise (e.g., via visual inspection) not be noticed.

The spatial distribution of temperatures can be analyzed as a raw radiance map produced by the thermal remote sensing instrument, or it can be further processed to obtain a calibrated surface temperature map. In the case of surface defect detection, a raw radiance map will suffice, as the main goal is to see relative differences in temperature between defective and intact areas, which will be revealed by either the radiance or true temperature image. Thermal remote sensing instruments usually consist of an array of thermal sensors similar to Charge Coupled Devices (CCD) or Complementary Metal Oxide Semiconductor (CMOS) sensors used in common photographic or video cameras, but sensitive to the thermal infrared part of the spectrum (see Figure 6). Such

thermal cameras produce digital images of the surface being monitored, with each pixel of the image representing a radiance or a temperature.

The temperature and associated radiance differences seen in a thermal image arise from the way heat is transferred in and out of the concrete surface, following the fundamental laws of thermodynamics. A concrete surface at a different temperature than the surrounding environment will tend to equilibrate with that environment's temperature; if the concrete surface is at a lower temperature than the ambient air (e.g., during the morning as the air is quickly heated by solar radiation), it will start to heat up, raising its temperature in a tendency to equilibrate thermally with the environment. Conversely, if the concrete surface is at a higher temperature than the ambient air (e.g., after sunset as the air quickly cools down), it will start to cool down, lowering its temperature again in a tendency to equilibrate thermally with the environment. In the case just discussed, the thermal energy is being transferred by conduction with the air in contact with the concrete (and by convection of the air), but an analogous situation can be considered for the case of thermal energy being transferred by radiation of electromagnetic energy. A surface being exposed to electromagnetic radiation will absorb part of that radiation (e.g., by the direct exposure to solar radiation), increasing its temperature, but it will also radiate energy according to the principles discussed in the previous section, losing energy and tending to cool down (e.g., after sunset). The balance between incident and radiated energy, and the thermal exchange with the surrounding air, will determine whether the surface will tend to heat or cool.

Structural defects and imperfections alter the heat transfer patterns (Maldague, 1993; Starnes, 2002; Washer, 2009). A delamination, which is basically a void in the concrete filled either with air or water, will conduct heat differently from the rest of the concrete structure. As the concrete temperature increases from the surface inwards (e.g., after sunrise), a delamination will act as a barrier slowing down heat transfer into the deeper parts of the concrete structure; this slowdown in heat transfer will result in an increase of the temperature of the concrete above the delamination. In the cases when concrete is cooling down (e.g., after sunset) the delamination acts again as a heat transfer barrier slowing down the heat flux, but in this case from the deeper parts of the concrete structure towards the surface, leading to a faster cooling of the areas above the delamination.

Practical applications of thermal remote sensing include both passive and active heat sources (Alqennah, 2000). Passive thermal remote sensing uses natural heat source, mainly solar heating, whereas active methods use artificial sources, like heat lamps and other heating devices. In both cases, it is necessary to have variations of the heating over time to allow for differences in heat transfer to highlight the anomalies (e.g., associated to delaminations). In the passive case the diurnal variation associated to insolation (from sunrise to sunset) provides that temperature change, and in the active case it depends on the time and mode of exposure to the heat source.

Asphalt and concrete pavement emissivity is usually assumed to be high (> 0.9), but this value can vary depending on the specific properties of the asphalt or concrete surface (e.g., how rough or smooth it is). More important, from a practical standpoint, is the possibility that other substances covering the concrete can dramatically change the surface emissivity, leading to very large differences in the calculated temperature (Clark et al. 2003). Although it may have an important impact on temperature measurements, emissivity may not be a critical variable in some cases where only relative differences of temperature (and therefore of radiance) are important. This occurs when the whole surface being measured has the same emissivity. Also important are other environmental variables that also control the heat transfer, like wind speed, which enhances convective and advective heat transfer (Washer et al. 2009; ASTM 2007).

Besides the characteristics of the concrete, the surface material covering the concrete, and the atmosphere, it is also important to consider the conditions of the potential defects that one is

attempting to be detect. The substance filling a delamination can have a large effect on heat transfer and therefore on potential detectability by thermal remote sensing. For instance, water will conduct heat much better than air (even at a similar rate than concrete); therefore, a water filled delamination may be much harder to detect by thermal methods (Maser and Roddis, 1990). The depth and width of the delaminations also play a key role in how heat is transferred to the surface, with deeper and thinner delaminations being harder to detect (Alqennah, 2000; Howard et al. 2010; Vaghefi et al. 2013). Finally, for passive thermal remote sensing the time of the day when the monitoring is done and the relationship to the insolation (the amount of solar radiation received by the surface) are also important. For example, the highest thermal contrast will be achieved at different times for delaminations at different depths, with deeper delaminations taking as much 7 hours to achieve maximum contrast (Washer et al. 2009).

Thermal remote sensing is seen as advantageous because it is a relatively fast and undisruptive monitoring technique that translates in shorter inspection and lane closure times (Maser and Roddis, 1990). The digital format of the thermal remote sensing instrument's output allows easy combination and integration of the monitoring information with other data platforms, including standard GIS software packages, allowing storage in a georeferenced database (Ahlborn et al. 2012).

2.2.3. Thermal inertia

Thermal imaging has shown great promise in detection of subsurface defects in concrete surfaces. However, a major challenge in interpreting thermal signatures is that shaded areas, presence of foreign material (e.g. paint, patches, hinges, and shaded areas) can produce similar thermal response as subsurface delaminations. This leads to false alarms. However, obtaining co-registered temperature difference maps taken during different times of the day (Repeat Pass Thermography) enable the computation of a thermal inertia map. Thermal inertia is a quantitative measure of the bulk resistance to temperature change which has shown to decrease in the presence of delaminations (DelGrande et al. 1996).

Thermal inertia (TI), with units of ($\text{J m}^{-2} \text{K}^{-1} \text{s}^{1/2}$), is traditionally described by the relationship

$$TI = \sqrt{\lambda \rho_b C} \quad \text{Equation 4.}$$

where λ is the thermal conductivity ($\text{W m}^{-1} \text{K}^{-1}$), ρ_b is the bulk density of the material (kg m^{-3}), and C is the specific heat capacity of the material ($\text{J kg}^{-1} \text{K}^{-1}$). However, when volumetric specific heat is used, which accounts for the bulk density, TI ($\text{J m}^{-2} \text{K}^{-1} \text{s}^{-1/2}$) can be represented by the following relationship:

$$TI = \sqrt{\lambda C_v} \quad \text{Equation 5.}$$

where C_v is the volumetric specific heat of the material ($\text{J m}^{-3} \text{K}^{-1}$). Repeat pass thermal remote sensing enables the computation of Apparent Thermal Inertia (ATI), which has been shown to be directly related to the thermal inertia (Minacapilli et al. 2012; Price 1985). ATI, with units of ($1/\text{K}$), is formulated as

$$ATI = \frac{1-\alpha}{\Delta T} \quad \text{Equation 6.}$$

where α is the surface albedo and ΔT is the change in temperature (K) from a diurnal heating cycle that can be determined by thermal imaging.

Studies have demonstrated that ATI is insensitive to surface clutter and can be effective in differentiating subsurface defects from surface clutter (Del Grande and Durbin 1999). This advancement could significantly reduce the false alarms and improve the accuracy in computing subsurface defects.

2.2.4. On-site monitoring vs. remote sensing and UAV based monitoring

The application of thermal remote sensing to roads and bridges is usually done from terrestrial vehicle setups, on which the thermal camera is mounted above the vehicle, aiming to cover the full width of the road lane, and the data acquisition is done as the vehicle drives on the road. The resolution of the acquired images (i.e., the size of the area covered by each pixel) depends on the camera sensor and optics and the distance at which it is positioned above the road surface, and limits the size of features that can be resolved on the thermal images.

UAVs allow for extra flexibility in imaging the road which cannot be achieved with conventional terrestrial vehicles, including the possibility to cover larger fields of view, operate with limited traffic interruptions, and image the fascia and underside of the bridges. Practical limitations to the UAV platform include maximum payload that they can carry, which constrains the size and weight of the chosen camera (and supporting hardware, like power supply, etc.), and which also limits flight time. Given all these variables, the tradeoff between them needs to be considered carefully to achieve a balance between the different goals and limitations that the different platforms and thermal remote sensing systems can achieve. Figure 7 shows an example of the tradeoffs that have to be considered when choosing a thermal sensor and platform system.

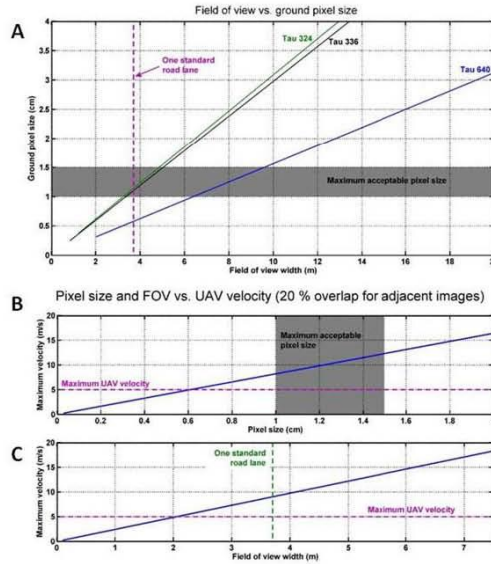


Figure 7. **A** Field of view vs. ground pixel size for three models of a FLIR Tau 2 thermal camera (models Tau 324, 336 and 640) with a 13 mm lens. Constraints on the minimum width of the field of view to be imaged (~ 3.7 m) and the maximum pixel size to detect significant delaminations (1 to 1.5 cm) are shown by the vertical magenta dashed line and the gray horizontal stripe, respectively. For thermal cameras mounted on a UAV, and in the case of a prime (fixed focal length or non-zoomable) lens both variables, field of view width and pixel size, will be controlled by the flying elevation above the ground. **B** Maximum UAV velocity vs. pixel size. As in panel A, some constraints are also shown in the graph, including the maximum UAV velocity for common UAV models (shown by the horizontal magenta dashed line) and the maximum pixel size (shown by the gray vertical stripe). **C** Maximum UAV velocity vs. field of view width, and again some constraints are shown in the graph, including the maximum UAV velocity for common UAV models (shown by the horizontal magenta dashed line) and the minimum field of view width (shown by the vertical green dashed line).

2.3. LiDAR

Light Detection and Ranging (LiDAR) is an optical remote sensing technology that determines distance to a target by measuring the time required for a laser pulse to travel to a target and return to the sensor (Vosselman and Maas 2010). A single laser pulse transmitted and received can only determine the distance and angle from the sensor to the target.

To define an object in three-dimensional space, the LiDAR scanner repeats the scanning process thousands of times per second. From the distance and the relative orientation of the laser pulse, the three-dimensional XYZ coordinates (or locations) associated with each measured pulse can be determined in relative space (Chu 2011). The dataset containing the XYZ coordinates and associated intensity values for these millions of sensed data points is commonly referred to as a point cloud. From this point cloud, a user can access and visually display the collected data in virtual space. Software can be used to manipulate and extract features of interest present within the data,

e.g., regions of high variation such as corners and objects. Compared to traditional surveying equipment, a LiDAR system can collect millions of XYZ data points in a single scan of a target, allowing a detailed 3D model of the scanned surface to be created.

LiDAR data is generally collected using one of three techniques, depending on project requirements: airborne, fixed and mobile terrestrial. The fundamental data scanning principles are the same, i.e., measuring the distance between the sensor and a target using lasers. The changes come in the hardware and software packages required to collect the data in a format appropriate for the desired use.

Airborne LiDAR uses a sensor mounted on or in an aircraft (manned helicopter or fixed wing aircraft or fixed wing, single- or multi-rotor UAV) that is designed to measure the distance between the airborne sensor and surface with a high degree of precision. LiDAR datasets collected using more recent hardware and software can also include data on return intensity and characterize multiple returns (which is important when imaging through foliage). The dataset generated by airborne LiDAR is often used to generate digital terrain or digital surface models, which describe the terrain over which the sensor is flown (Figures 8A and 8B).

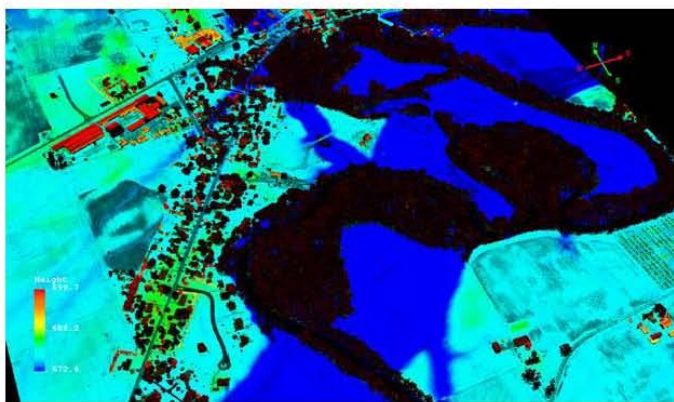


Figure 8A. Screen capture of a LiDAR point cloud with intensity information. The elevation colors are blue/low to red-high relative to this particular dataset. Black areas show regions of low return intensity. Note the additional information available using the information from return intensity compared to elevation only (below).

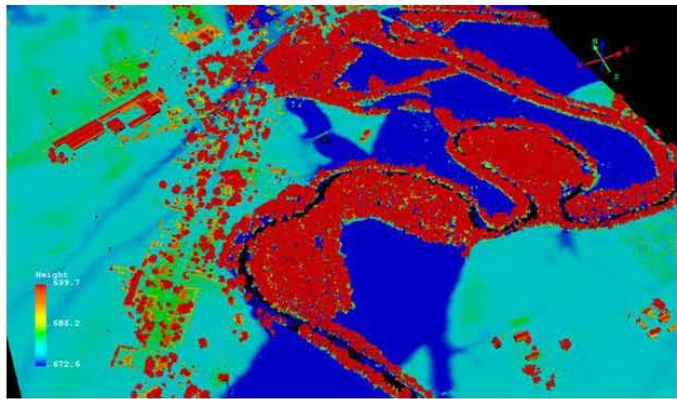


Figure 8B. Screen capture of return elevation only data. Relative point cloud elevations are clear but much information is missing compared to the intensity enabled image (Figure 8A).

LiDAR is an active remote sensing technology, meaning that no other illumination source (such as the sun) is required. LiDAR data can be collected during off-hours – mid-day, evening or night based on project specific considerations. Generally, the datasets collected by manned airborne platforms cover a relatively large area at moderate (0.5-5 m) post spacing (the average distance between LiDAR pulses on the surface). Large areas can be scanned relatively quickly, but the point of view of an airborne scanner is straight down – the sides of structures are generally not part of the dataset.

LiDAR works by illuminating a target with a laser pulse and measuring the amount of time it takes for the pulse to return to the sensor to determine the distance to the target. This measurement technique is known as time-of-flight. Laser rangefinders use the same method of measurement, but rather than making a single distance measurement, terrestrial LiDAR scanners utilize spinning mirrors and a rotating base to collect millions of measurements over a scene (CFLHA 2011).

LiDAR scanners generally use two techniques used to measure distance. Time-of-flight (TOF), discussed briefly above is one, and phase shift, where a continuous, sinusoidally modulated laser beam is transmitted from the scanner is the other (Flood 2001). The distance to the target is calculated by comparing the phase of the returned pulse with the transmitted pulse. TOF LiDAR scanners measure the time it takes for a laser pulse to travel to and from the target. A simple calculation is then automatically performed within the data acquisition and control system to determine an object's distance from the receiver. The calculation for determination of the travel distance of a pulse is

$$\text{Distance} = (\text{speed of light}) \times (\text{time of flight})/2. \quad \text{Equation 7-1}$$

TOF scanners have multiple modulation frequencies that are utilized to increase the measurement accuracy. Additionally, TOF scanners can be used to measure different data sets bounded by the return time of the pulse. This feature is primarily used in forestry applications allowing for the generation of both a canopy profile with the “first return” and a ground surface profile with the “last return” (Reutebuch et al. 2005).

In phase-shift units, a continuous laser beam with sinusoidally modulated optical power is projected from the transmitter and reflected off the suspect object. The reflected radiation wave is then sensed by the receiver and compared to the original emitted radiation to determine the present phase shift within the acquired data. Once the phase shift is determined, the TOF is then automatically calculated by

$$\text{Time of Flight} = (\text{Phase Shift}) / 2 \pi \times (\text{Modulation Frequency}) \quad \text{Equation 7-1}$$

The distance to the target is then calculated by substituting the determined TOF from Equation 7-2 into Equation 7-1. TOF sensors are often used for longer range exterior survey and civil engineering applications such as roadway/bridge as-built surveys and mobile scanning applications. The working range of TOF sensors can extend to more than 250 m, depending on the requirements of the data collection. Phase-based sensors have a working range of around 80 m and are frequently used for as-built surveys of refineries/manufacturing plants and interior architectural spaces where distances to be measured are shorter. Data collection using LiDAR requires an unobstructed path between the scanner and the target (note that multiple return LiDARs do have some ability to scan through foliage and other “transparent” objects).

When a LiDAR pulse reaches an opaque object (whether it is the desired target or not), some of the pulse is reflected back to the sensor. Nothing behind the object is ‘visible’ to the sensor. The line of sight nature of LiDAR highlights a potential issue - if the target has many occluding surfaces, “shadows” or “blind spots” in the instrument’s FOV (field-of-view) can occur. The line-of-sight issue can be resolved by repositioning the device to allow the shadowed surfaces of the complex object to be revealed. By combining the multiple point clouds collected from each scan, a three-dimensional rendering of the object can be created by fusing together data from multiple collection views. LiDAR returns usually include multiple attributes which can include RGB (red, green, and blue) and intensity (brightness) values in addition to XYZ location information.

Miller et al. (1998) proposed the first proof-of-concept platform for UAV-based LIDAR and since then several other capable micro-UAV platforms have been developed, which address this task (Choi et al., 2009, Nagai et al., 2009, Jaakkola et al., 2010, Lin et al., 2011). Until recently, however, size and budget were significantly larger than most real-world organizations could afford. The UAVs developed by Choi, Nagai, and Jaakkola were very large and used tactical grade IMUs and laser scanners (costing >\$50,000 typically). Two LIDAR UAV platforms that use lower cost components include those developed by Serrano (2012) and Wallace et al. (2012).

Serrano’s (2012) work on culvert inspection and Wallace’s (2012) work in taking forest inventory are perhaps the most advanced LIDAR-based micro-UAV systems. Each system used a multicopter platform (e.g., quadcopter or hexacopter). Serrano’s system is based on the Ascending Technologies Pelican platform, as seen in Figure 9. Their 3D point cloud is built by fusing together information from an internal inertial mapping unit (IMU), an onboard GPS receiver, and a Hokuyo UTM-30LX LIDAR sensor (the same sensor used in our demonstration system). The 3D point cloud data of the culvert is post-processed by using the IMU / GPS sensor for initial position and pose estimation together with a scan matching algorithm which matches up two consecutive laser scans with the assumption that the objects viewed have not changed or moved in the small amount of time between scans. Although Serrano’s work is theoretically exciting, the results are inconclusive in how well the system could be used for culvert inspection. The conclusion of the thesis indicates that “it would be possible to use the LIDAR to construct a point cloud of the 3D shape of the (culvert) opening.” As a proof of concept, it can help inform the recent state of the practice.



Figure 9. Ascending Technologies Penguin.

In Wallace's (2012) system, they developed a sensor package for an optocopter that fused an IMU, a GPS, and a high definition (HD) camera. The platform is shown in Figure 10. The IMU / GPS system measured rough position and pose estimates while the camera was used with structure-from-motion algorithms to detect the horizontal (and vertical, to a degree) motions of the platforms. Their system did not use a scan matching algorithm to further reduce the error of the 3D point cloud estimation. However, they were able to show that the inclusion of video information reduced horizontal accuracy from 0.61 meters to 0.34 meters (root mean square error or RMSE). The standard deviation of tree height, as estimated by their system, was 0.26 meters, with a data density of 8 points per square meter. 15 centimeter accuracy was achievable when more points per tree crown were available. Lastly, the RMSE in tree location was 0.53 meters, and RMSE in crown width was 0.61 meters. Figure 11 shows an example of the point cloud produced by their method. In summary, this shows that that a LIDAR system on a micro-UAV is able to achieve RMSE values on the order of 10-50 centimeters (depending on the measurement) when using a fused IMU/GPS and camera structure-from-motion system.

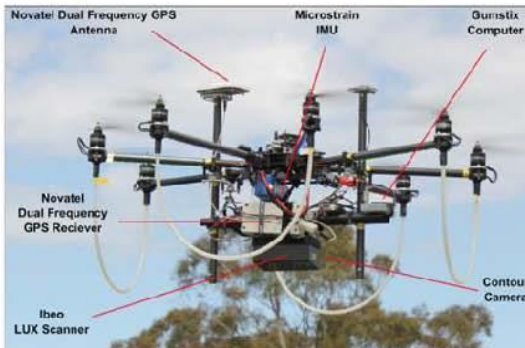


Figure 10. Wallace et al. (2012) forest inventory optocopter platform.

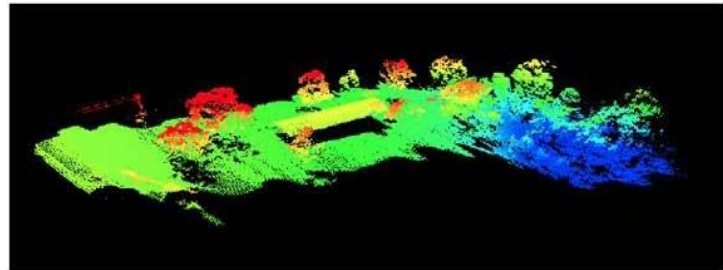


Figure 11. An example point cloud produced by Wallace et al. (2012).